

Doctorate Dissertation

博士論文

Development of an *in vitro* human liver model by using iPS cells

(ヒト iPS 細胞を用いた肝臓モデルの構築)

A Dissertation Submitted for Degree of Doctor of Philosophy

December 2018

平成 30 年 12 月博士 (理学) 申請

**Department of Biological Sciences, Graduate School of Science,
The University of Tokyo**

東京大学大学院理学系研究科生物科学専攻

Yuta Kouji

厚井悠太

Table of Contents

List of Abbreviations	3
Abstract	4
Introduction	5
Material and Methods	9
Results	18
Discussion	29
Conclusion	34
References	35
Figures and Tables	40
Acknowledgements	78

List of Abbreviations

AFP: Alpha fetoprotein
ALB: albumin
ALCAM: Activated leukocyte cell adhesion molecule
APC: Allophycocyanin
BMP: Bone Morphogenetic Protein
CPM: Carboxypeptidase M
ECM: Extra cellular matrix
EGF: Epidermal growth factor
FCGR2: Fc fragment of IgG receptor II
FCM analysis: Flow-cytometric analysis
FGF: Fibroblast growth factor
FITC: Fluorescein isothiocyanate
F8: Factor VIII
HGF: Hepatocyte growth factor
hiPSC: human induced pluripotent stem cell
HSC: Hepatic stellate cell
HUVEC: Human umbilical vein endothelial cell
LPC: Liver progenitor cell
LSEC: Liver sinusoidal endothelial cell
MEF: Mouse embryonic fibroblast
MSC: Mesenchymal stem cell
NPC: Non-parenchymal cell
OSM: Oncostatin M
PE: Phycoerythrin
RNA-seq analysis: RNA sequencing analysis
STM: septum transversum mesenchyme
TGF β : Transforming growth factor β
UV: Ultraviolet
VEGF: Vascular endothelial growth factor

Abstract

During liver development, hepatoblasts and liver non-parenchymal cells (NPCs) such as liver sinusoidal endothelial cells (LSECs) and hepatic stellate cells (HSCs) constitute the liver bud where they proliferate and differentiate. Accordingly, I reasoned that liver NPCs would support the maturation of hepatocytes derived from human induced pluripotent stem cells (hiPSCs), which usually exhibit limited functions. I found that the transforming growth factor β and Rho-ROCK signaling pathway, respectively, regulated the proliferation and maturation of LSEC and HSC progenitors isolated from mouse fetal livers. Based on these results, I have established culture systems to generate LSECs and HSCs from hiPSCs. These hiPSC-derived NPCs exhibited their distinctive phenotypes and promoted self-renewal of hiPSC-derived liver progenitor cells (LPCs) over the long term in the two-dimensional culture system without exogenous cytokines and hepatic maturation of hiPSC-derived LPCs. In the co-culture system of LPCs and NPCs derived from iPS cells, hepatocytes expressed a number of liver enzymes at levels comparable to those cultured primary human hepatocyte. Thus, a functional human liver model can be constructed *in vitro* from the LPCs, LSECs, and HSCs derived from hiPSCs.

Introduction

The function and structure of the liver

The liver is the largest internal organ and a central organ for homeostasis exhibiting various functions, including metabolism of nutrients, production of bile, and detoxification. Parenchymal cells, or hepatocytes are the major cell type that expresses various metabolic enzymes such as a number of cytochrome P450 oxidases responsible for the biotransformation of various compounds as well as drugs. Other liver cells, such as liver sinusoidal endothelial cells (LSECs), hepatic stellate cells (HSCs), biliary epithelial cell known as cholangiocytes, and Kupffer cells, are called non-parenchymal cells. LSECs and HSCs constitute liver sinusoids, which is a microvasculature in the liver (Figure 1). LSECs compose the wall of sinusoids and serve as a filter of substance supplied to hepatocytes. LSECs have a number of specialized features including the presence of multiple fenestrations in the healthy liver. This morphological feature allows open access for solutes between blood and hepatocytes. HSCs reside in a space of Disse between hepatocytes and LSECs. HSCs play key roles for maintaining concentration of vitamin-A in the blood as vitamin-A storage cells, and modulate blood circulation of liver sinusoids. Cholangiocytes compose the bile duct, which drains bile produced by hepatocytes. Kupffer cells are the resident macrophage located in the liver sinusoids and play critical roles in the innate immune response.

The liver is organized into lobules, functional and structural units of the liver (Figure 1).

Lobules are the hexagonal structure around the central vein, and the portal vein is located in outer corners of the lobules. Blood from intestine enters the liver through the portal vein and flows to central vein through liver sinusoid.

Although hepatocytes play roles for most of liver functions, recent studies have revealed that various liver functions are supported by interactions between parenchymal cells and non-parenchymal cells. Moreover, formation of lobule structure allows hepatocytes to sustain various metabolic functions.

Liver development

Hepatoblasts are the embryonic liver progenitor cells (LPCs) derived from foregut endoderm and defined as the cell with the potential to differentiate to both hepatocytes and cholangiocytes. In mice, liver development starts with the hepatic specification of the foregut endoderm at embryonic day 8.5-9.0 of gestation (E8.5–E9.0) (Tremblay and Zaret, 2005). Hepatoblasts proliferate and migrate into the septum transversum mesenchyme (STM) derived from mesoderm to form the liver bud. Hepatoblasts become mature hepatocytes and cholangiocytes through interactions with hepatic non-parenchymal cells (NPCs) such as liver sinusoidal endothelial cells (LSECs) and hepatic stellate cells (HSCs) derived from STM (Figure 2). Previous studies showed impaired hepatic differentiation in mutant mice lacking LSECs or HSCs (Hentsch et al., 1996; Matsumoto et al., 2001), revealing important roles for NPCs in liver development. Although the mechanism by which NPCs induce hepatic maturation is not understood

completely, LSECs support the growth of liver bud and to supply nutrients by constructing microvasculars. HSCs particularly secreted a number of hepatic mitogens, such as HGF, Wnt9a, pleiotrophin, and FGF10 during embryogenesis (Yin et al., 2013).

Human induced pluripotent stem cell-derived hepatocyte

Primary cultures of human hepatocytes have been used for drug discovery and toxicology. However, because hepatocytes lose their function after isolation from the body, primary cultured hepatocytes exhibit very limited metabolic activity. Additionally, the supply of human hepatocytes is also limited and it is almost impossible to obtain the same sample repeatedly over the long term. To overcome these problems, human embryonic stem cells (hESCs) and human induced pluripotent stem cells (hiPSCs) are considered as an alternative cell source for production of hepatocytes.

Human induced pluripotent stem cells (iPSCs) can be generated from a variety of somatic cells and have been used as an alternative cell source for production of different types of human cells (Takahashi et al., 2007). Several protocols have been reported for generation of hepatocytes from iPSCs (Ogawa et al., 2013; Si-Tayeb et al., 2010; Takayama et al., 2012). However, differentiation of hepatocytes from iPSCs requires time-consuming multiple costly processes, and also iPSC-derived hepatocytes exhibit immature phenotypes with limited functions. In our laboratory, a method was established to isolate liver progenitor cells (LPCs) by using carboxypeptidase M (CPM) as a cell-surface marker for LPCs. (Kido et al., 2015; Tanaka et al., 2007). CPM⁺ LPCs

derived from hiPSCs were shown to have potential to proliferate and differentiate into both hepatocyte-like and cholangiocyte-like cells (Kido et al., 2015). While hepatocytes derived from CPM⁺ LPCs exhibit much higher metabolic activity compared with those derived from hiPSCs using a conventional protocol, the levels of some mature hepatic functions are still not as high as those in primary human hepatocytes.

hiPSC-derived human liver model

Because hepatocyte function is maintained by LSECs and HSCs in our body and induced by signaling from non-parenchymal cells in the liver development, it is necessary to develop co-culture system by parenchymal cells and non-parenchymal cells for generating mature hepatocytes *in vitro*. As an initial step for generation of hiPSC-derived liver models, my aim was to generate LSECs and HSCs capable of supporting the proliferation and differentiation of LPCs. In the present study, to develop an efficient culture system of LSECs and HSCs from hiPSCs, I searched and identified cell surface molecules for isolation of LSEC and HSC progenitors during mouse liver development. Then, I established culture systems for expansion and differentiation of these progenitors. According to a mouse study, I newly developed an efficient culture system for hiPSC-derived LSECs and HSCs. These hiPSC-derived NPCs exhibited specific cell function and supported LPC proliferation and maturation.

Materials and Methods

Mice

C57BL/6 mice were purchased from CLEA Japan, Inc (Tokyo, Japan). All mouse experiments were performed according to the guidelines of the institutional Animal Care and Use Committee of the University of Tokyo.

Isolation of LSEC progenitors and HSC progenitors from fetal mouse livers

LSEC and HSC progenitors were isolated from livers of E12.5 fetal mice. The fetal livers (each sample contained 25-35 embryos) were minced and dissociated in Liver Digest Medium (Life Technologies, California, US) for 10 minutes at 37°C. The fetal liver cell suspension was hemolyzed and passed through a 70 µm cell strainer (BD Biosciences, New Jersey, US). Then, cells were treated with FcR blocking reagent for 20 minutes to reduce non-specific antibody binding and incubated with specific antibody against cell surface protein such as FITC-conjugated anti-CD31 antibody (BD Biosciences), PE-conjugated anti-FLK1 antibody (eBioscience, San Diego, USA), biotin-conjugated anti-CD34 antibody (eBioscience), APC-conjugated anti-ALCAM antibody (eBioscience), or BUV395- or BV711-conjugated anti CD45-antibody (BD Biosciences) for 30 minutes on ice. Cells were then washed and labeled with streptavidin APC or streptavidin BV421 (BD Biosciences). CD45⁻CD31⁺FLK1⁺CD34⁺ cells and CD45⁻ALCAM^{high} cells were isolated by a MoFlo XDP cell sorter (Beckman Coulter, Inc, California, US). Antibodies are listed in Table 1.

Human iPS cell culture

The hiPSC line, 454E2 and 409B2, were provided by RIKEN Cell Bank (Okita et al., 2011), and TkDN4-M was obtained from the Institute of Medical Science, the University of Tokyo (Takayama et al., 2010). hiPSCs were maintained on mitomycin C-treated (Wako Pure Chemicals Industries, Osaka, Japan) mouse embryonic fibroblast (MEF) feeder cells. hiPSC-derived NPCs were induced from 454E2, 409B2, and TkDN4-M cell lines. hiPSC-derived LPCs were prepared from the TkDN4-M cell line according to previous protocol (Kido et al., 2015).

Differentiation of HSCs from human iPS cells

Prior to differentiation, human iPS cells were dissociated into small clusters, and MEF feeder cells were depleted by replating on gelatin-coated plates for 30 minutes at 37°C. To induce mesoderm differentiation, the small clusters were collected and cultured on Ultra-Low Attachment plates (Corning, New York, US) in Stempro-34 SFM medium; supplemented with Y27632 (10 μ M) and BMP4 (2 ng/ml) (day 0 to day 1), Activin A (5 ng/ml), bFGF (5 ng/ml), and BMP4 (30 ng/ml) (day 1 to day 4), VEGF (10 ng/ml), SB431542 (5.4 μ M), and Dorsomolphen (0.5 μ M) (day 4 to day 6). All cell cultures were maintained in a 5% CO₂, 4% O₂ environment. After 6 days of culture, ALCAM^{high} HSC progenitors were isolated using a MoFlo XDP cell sorter. They were plated onto plates coated with collagen Type I-C at the density of 15000 cells/cm² in HSC medium: MSCGM supplemented with Y27632 (10 μ M). To induce maturation for HSCs,

ALCAM^{high} HSC progenitors were cultured for 5-6 days in HSC medium under 5% CO₂, 20% O₂. Reagents are listed in Table 2.

Differentiation of LSECs from hiPSCs

In order to induce LSEC progenitors, after 6 days of cultures for mesoderm induction using the same protocol as HSC induction, total mesodermal cell clusters were transferred onto gelatin coated plates and cultured in Endothelial cell (EC) medium: EGM-2 supplemented with VEGF (50 ng/ml), and cultured for 7 days. After enrichment using autoMACS Pro Separator (Miltenyi Biotech), CD31⁺FLK1⁺CD34⁺ LSEC progenitors were isolated using a MoFlo XDP cell sorter. They were cultured on fibronectin-coated plates in EC medium. When the cells reached subconfluent, to induce LSECs, CD31⁺FLK1⁺CD34⁺ LSEC progenitors were dissociated using 0.05% trypsin/0.5 mM EDTA solution and replated on a fresh dish at the density of 15000 cells/cm² in LSEC differentiation medium: EC medium supplemented with A83-01 (1.5 μM). After 14 days of culture, CD31⁺FCGR2⁺ LSECs were enriched by a MoFlo XDP cell sorter. All cell cultures were maintained under 5% CO₂, 4% O₂ environment.

Co-culture of hiPSC-derived LPCs on hiPSC-derived NPC feeder cells

To expand hiPSC-derived LPCs, LPCs were cultured on mitomycin C-treated (Wako) HUVEC/MSC or hiPSC-derived NPC (LSEC and HSC) feeder cells (50,000 cells/cm²) in DMEM/F12 supplemented with 10% fetal bovine serum, penicillin-streptomycin-glutamine, insulin-transferrin-selenium, N2 supplement, MEM

non-essential amino acids solution, L-glutamine, ascorbic acid (1 mM), nicotinamide (10 mM), N-acetylcysteine (0.2 mM), dexamethasone (1×10^{-7} M), Y27632 (5 μ M), and A83-01 (2.5 μ M) for 14 days. To induce hepatic maturation of hiPSC-derived LPCs, cells were cultured in HBM supplemented with HCM SingleQuots (excluding epidermal growth factor) and oncostatin M (20 ng/mL) for 5 days. Reagents are listed in Table 2.

High-density co-culture system of hiPSC-derived LPCs and NPCs

hiPSC-derived CPM⁺ LPCs (20,000 cells/well), hiPSC-derived LSECs (20,000 cells/well), and hiPSC-derived HSCs (20,000 cells/well) were plated onto collagen Type I-A gel in a 48-well plate. Cells were cultured in DMEM/F12 supplemented with 10% FBS, penicillin-streptomycin-glutamine, insulin-transferrin-selenium, N-2 supplement, MEM non-essential amino acids solution, L-glutamine, ascorbic acid (1 mM), nicotinamide (10 mM), N-acetylcysteine (0.2 mM), dexamethasone (1×10^{-7} M), Y27632 (5 μ M), and A83-01 (2.5 μ M), HGF (20 ng/ml), EGF (10 ng/ml), and OSM (20 ng/ml) for 10 weeks. Reagents are listed in Table 2.

Induction of vasculogenesis

Induction of vasculogenesis *in vitro* was performed using the three-dimensional culture system. hiPSC-derived LSECs (200,000 cells) and HSCs (20,000 cells) were suspended in 50 μ l gel of 2:3 mixture of GFR matrigel and collagen Type I-A. Cell were plated onto 24-well plate and incubated for 30 minutes. After solidification, LSEC medium

was added, and cells were cultured for 14 days. Reagents are listed in Table 2.

Induction of liver organogenesis

Induction of liver organogenesis *in vitro* was performed using the three-dimensional culture system. hiPSC-derived LPCs (80,000 cells), LSECs (200,000 cells), and HSCs (40,000 cells) were resuspended and plated on oxygen-permeable PDMS-based honeycomb microwells (Shinohara et al., 2017). Cells were cultured in DMEM/F12 supplemented with 10% FBS, penicillin-streptomycin-glutamine, insulin-transferrin-selenium, N-2 supplement, MEM non-essential amino acids solution, L-glutamine, ascorbic acid (1 mM), nicotinamide (10 mM), N-acetylcysteine (0.2 mM), dexamethasone (1×10^{-7} M), Y27632 (5 μ M), and A83-01 (2.5 μ M), HGF (20 ng/ml), EGF (10 ng/ml), bFGF (10 ng/ml), and VEGF (50 ng/ml) for 1 week. Reagents are listed in Table 2.

Human cell culture

HUVECs and human MSCs were purchased from Lonza. Human primary hepatocytes were purchased from Biopredic International (Rennes, France). Human primary LSECs were purchased from Cell Systems Corporation (Washington, US) and ScienCell Research Laboratories (California, US). Human primary HSCs were purchased from Zen-Bio (North Carolina, US) and ScienCell Research Laboratories. These cells were cultured according to the manufacturer's protocol.

Isolation of hiPSC-derived LSEC and HSC progenitors and mature LSECs

Cell clusters were collected and dissociated into single cells using Accumax Cell Dissociation Solution (Innovative Cell Technologies, San Diego, US). Cultured cells were dissociated using 0.05% trypsin/0.5 mM EDTA solution. Cells were resuspended in PBS containing 0.03% BSA, then were incubated with FcR blocking reagent (Miltenyi Biotech) followed by incubation with appropriate fluorescent conjugated antibodies specific for LSEC progenitors, HSC progenitors, or mature LSECs. Cell populations of interest were isolated by using a MoFlo XDP cell sorter. Antibodies are listed in Table 1.

Flow cytometric analysis for cytosolic protein

Intracellular staining was performed using Cytofix/Cytoperm Fixtation/permeabilization kit (BD Biosciences) according to the manufacture's protocol. Antibodies are listed in Table 1.

Monitor of cell growth

hiPSC-derived or fetal mouse liver-derived cells were seeded into each well. Cells were counted in triplicate using a hemocytometer.

Vitamin A uptake assay

Cells were incubated with 10 μ M retinol (Sigma-Aldrich Corporation, St. Louis, US) for 24 hours at 37°C. Then, they were dissociated using 0.05% trypsin/0.5 mM EDTA

solution, and autofluorescence of intracellular Vitamin A droplets was detected by using FACSCanto II or MoFlo XDP cell sorter (BD Biosciences). Reagents are listed in Table 2.

Quantitative RT-PCR

Total RNA was extracted using TRIzol reagent (Life Technologies) or NucleoSpin RNA XS (MACHEREY-NAGAL, Duren, Germany) according to the manufacture's protocol. Residual genomic DNA was digested with DNase I (Life Technologies). First-strand cDNA was synthesized using PrimeScriptII 1st strand cDNA Synthesis Kit (Takara bio, Shiga, Japan). Quantitative RT-PCR was performed using SYBR Premix EX TaqII (Takara bio). All data were calculated using the ddCt method with β -actin as a normalization control. Primers are listed in Table 3.

Immunocytochemistry

Cultured cells were fixed in 10% buffered formalin solution (Wako Pure Chemical Industries, Ltd.) for 10 minutes and permeabilized with 0.2% Triton-X 100 (Wako Pure Chemical Industries, Ltd.) for 15 minutes. The cells were blocked with 5% skim milk (BD Biosciences) for 30 minutes and incubated with primary antibodies at 4°C overnight. After washing three times with PBS, cells were incubated with fluorescein-conjugated secondary antibodies and counterstained with Hoechst33342. Antibodies are listed in Table 1.

HGF, AFP, and ALB assay

HGF, AFP, and ALB levels in the culture supernatant were measured by Human HGF Quantikine ELISA Kit (R&D Systems, Minneapolis, US), AFP Human ELISA Kit (abcam), and ALB Human ELISA kit (abcam) according to manufacturer's protocol.

Microarray analysis

Total RNA was extracted with RNeasy Mini Kit (Qiagen, California, US) according to the manufacture's protocol. Whole human gene expressions were determined by microarray analysis using SurePrint G3 Human Gene Expression 8x60K v3 (Agilent Technologies). Heat maps were drawn based on the normalized gene expression data. The accession number for the microarray data reported in this study is GEO: GSE92771.

RNA-seq analysis

Total RNA was extracted using TRIzol reagent (Life Technologies) according to the manufacture's protocol. Libraries were prepared using the Illumina TruSeq Stranded Total RNA with Ribo-Zero Kit. All libraries were sequenced using an Illumina HiSeq 2000. The mapping of the reads was performed using the STAR program and the RSEM program was used to quantify transcripts. Heat maps were drawn based on the TPM value using MeV version 4.8.1. The accession number for the RNA-seq data reported in this study is GEO: GSE98710.

Data Analysis

The F test was performed to evaluate equal variance in the data. Significant differences were determined by Student's two-tailed t test or Welch's two-tailed t test depending on scedasticity. One-way ANOVA followed by Tukey's test was used to determine significant differences between more than two groups.

Results

Isolation of LSEC progenitors and HSC progenitors from mouse fetal livers

Because LSEC progenitors and HSC progenitors are present in the fetal liver bud where they proliferate and differentiate into mature LSECs and HSCs, respectively, it would be useful if such cells could be derived from hiPSCs. In order to establish culture systems for LSEC progenitors and HSC progenitors, I searched for cell-surface molecules that would be useful for the identification and isolation of these progenitors. It has been reported that LSEC progenitors express endothelial markers such as FLK1, CD31, and CD34 (Nonaka et al., 2007), and ALCAM⁺ septum transversum mesenchymal cells were shown to give rise to HSCs during fetal liver development (Asahina et al., 2011). As shown in Figure 3, flow-cytometric (FCM) analysis showed that CD45⁻FLK1⁺ endothelial cells and CD45⁻ALCAM^{high} mesenchymal cells were clearly detected in the fetal livers at E12.5, and I found that CD45⁻FLK1⁺ endothelial cells also expressed CD31 and CD34. Consistently, qRT-PCR analysis showed that CD45⁻FLK1⁺CD31⁺CD34⁺ cells isolated from fetal livers expressed LSEC marker genes such as *Stab2* and *Lyve1* (Figure 4A), suggesting that they are LSEC progenitors. On the other hand, CD45⁻ALCAM^{high} cells expressed HSC marker genes such as *Des*, *Ngfr*, *Cygb*, and *Lrat* (Figure 4A), suggesting that they are HSC progenitors. FCM analysis of fetal liver cells revealed the presence of CD45⁻ALCAM^{low} cells (Figure 3). As ALCAM has been reported to be weakly expressed in hepatoblasts (Asahina et al., 2009), I examined whether CD45⁻ALCAM^{low} cells expressed hepatoblast markers and

revealed that they expressed *Hnf4a*, *Afp*, and *Alb* (Figure 4B), indicating that they are hepatoblasts. These results suggest that a combination of these specific cell-surface markers could be used to enrich for LSEC progenitors and HSC progenitors from differentiating hiPSCs.

Development of efficient culture systems for LSEC progenitors and HSC progenitors

To produce large quantities of mature LSECs and HSCs, I sought to establish culture systems that allow the expansion and maturation of CD45⁻FLK1⁺CD31⁺CD34⁺ LSEC progenitors and CD45⁻ALCAM^{high} HSC progenitors, which were isolated from mouse fetal livers. Importantly, CD45⁻FLK1⁺CD31⁺CD34⁺ LSEC progenitors were highly proliferative (Figure 5), and maintained their characteristics after expansion *in vitro* (data not shown). Because our laboratory revealed that transforming growth factor β (TGF β) signaling inhibits maturation of LSECs from mouse embryonic stem cells (Nonaka et al., 2008), I then evaluated the differentiation potential of expanded CD45⁻FLK1⁺CD31⁺CD34⁺ LSEC progenitors. After induction of LSEC maturation by inhibiting TGF β signaling using A83-01, a TGF β RI inhibitor, in the hypoxic culture, mature LSEC-specific markers such as *Stab2*, *F8*, and *Lyve1* were highly upregulated compared with the control without A83-01 (Figure 6). I evaluated the effects of other TGF β RI inhibitors, such as SB431542 and LY364943, in LSEC maturation. However, these inhibitors were not effective in LSEC maturation compared with A83-01 (data not shown). On the other hand, signals for survival and differentiation of HSC progenitors

have not been elucidated. Although the Rho-ROCK signaling pathway was reported to play a role in the activation of mature HSCs (Murata et al., 2001), its effect on HSC progenitors was unknown. I assessed the role of the Rho-ROCK signaling pathway in CD45⁻ALCAM^{high} HSC progenitors by Y27632, a potent ROCK inhibitor, and found that they proliferated in the presence of Y27632 (Figure 7). Moreover, after cultivation in the presence of Y27632, the cells highly expressed mature HSC marker genes such as *Hgf*, *Cygb*, and *Lrat* (Figure 8). As basic fibroblast growth factor (bFGF) and oncostatin-M (OSM) were identified as key molecules for proliferation and differentiation of hepatic mesenchymal cell (Onitsuka et al., 2010), I evaluated the effects of these molecules on HSC maturation. However, HSC marker genes were not up-regulated in the presence of bFGF and OSM (data not shown). These results suggested that the Rho-ROCK signaling pathway regulates the proliferation and maturation of HSC progenitors. Taken together, these data demonstrated that FLK1⁺CD31⁺CD34⁺ LSEC progenitors and ALCAM^{high} HSC progenitors could be expanded *in vitro* while maintaining their potential to become mature cells (Figure 9).

Generation of LSEC progenitors from hiPSCs

To develop an efficient culture system for producing mature LSECs from hiPSCs, I attempted to generate LSEC progenitors capable of proliferating and differentiating into mature LSECs *in vitro*. It is well established that endothelial cells arise from mesodermal cells during embryogenesis. Likewise, LSEC progenitors are considered to have arisen from mesodermal cells. Therefore, I developed a differentiation system for

LSEC progenitors after the induction of hiPSCs into mesodermal cells according to the published protocol with some modifications (Kattman et al., 2011; White et al., 2013) (Figure 10). I assessed the differentiation of hiPSCs by qRT-PCR analysis. The expression of the pluripotency marker gene, *OCT4*, was decreased, whereas the expression of the mesodermal marker, *MESPI*, was increased along with mesodermal differentiation (Figure 11). The endothelial marker genes, *CD31* and *CDH5* (VE-cadherin), were highly expressed in hiPSC-derived cells at the endothelial progenitor stage (Figure 11). Surprisingly, the LSEC marker genes, *STAB2* and *LYVE1*, were also upregulated at this stage (Figure 11). I therefore tested whether FLK1⁺CD31⁺CD34⁺ LSEC progenitors were generated in the culture. Interestingly, FCM analysis showed that FLK1⁺CD31⁺CD34⁺ and FLK1⁺CD31⁺CD34⁻ cells were already present in the differentiation stage by this culture system (Figure 12A). To further characterize these cells, I isolated CD34⁺ and CD34⁻ fractions and analyzed their gene expression patterns. Sorted FLK1⁺CD31⁺CD34⁺ cells highly expressed LSEC-specific genes such as *STAB2*, *LYVE1*, and *FLT4* compared with pre-sorted cells and FLK1⁺CD31⁺CD34⁻ cells (Figure 12B). On the other hand, the FLK1⁺CD31⁺CD34⁻ cell population highly expressed pluripotent marker and mesenchymal markers compared with the FLK1⁺CD31⁺CD34⁺ cell population (data not shown). These results suggested that FLK1⁺CD31⁺CD34⁺ cell derived from hiPSCs exhibit characteristics of LSEC progenitors in the mouse fetal liver. FLK1⁺CD31⁺CD34⁺ LSEC progenitor cells derived from hiPSCs proliferated and exhibited morphology similar to that of endothelial cells (Figures 13A). These cells were highly proliferative (Figure 13B) and

could be expanded for several passages (Figure 13C). Furthermore, serially cultured cells maintained high expression levels of the LSEC progenitor markers, *FLK1*, *CD34*, *CD31*, *CDH5*, *STAB2*, and *LYVE1* (Figure 13D). Additionally, they could be cryopreserved without phenotypic changes (Figure 14). Collectively these data indicated that FLK1⁺CD31⁺CD34⁺ cells derived from hiPSCs are LSEC progenitors.

Maturation of LSECs from hiPSC-derived LSEC progenitors

As FLK1⁺CD31⁺CD34⁺ LSEC progenitors from fetal mouse livers differentiated into mature LSECs by inhibiting TGFβ signaling in hypoxic culture conditions (Figure 6), I investigated whether hiPSC-derived LSEC progenitors undergo functional maturation in our culture system (Figure 10). After culturing in the presence of A83-01 under hypoxic conditions for 14 days, the expression levels of the mature LSEC markers, *FCGR2B*, *STAB2*, *F8* (Factor VIII), and *LYVE1*, were highly upregulated (Figure 15). Because FCGR2 was detected only in mature LSECs from adult mouse livers (Nonaka et al., 2007), I enriched the CD31⁺FCGR2⁺ population by using a cell sorter and considered them as hiPSC-derived mature LSECs (Figure 16A). qRT-PCR analysis showed that the LSEC-specific marker genes, *FCGR2B*, *STAB2*, and *F8*, were highly expressed in CD31⁺FCGR2⁺ LSECs compared with CD31⁺FCGR2⁻ cells and human umbilical vein endothelial cells (HUVECs) (Figure 16B). In addition, these expression levels were comparable with or much higher than those in primary human LSECs. Isolated CD31⁺FCGR2⁺ mature LSECs could also be cultured for several passages and exhibited typical mature endothelial morphology (Figure 17A). Immunohistochemical and FCM

analysis showed strong expression of F8, a specific marker of mature LSECs (Figures 17B and 17C). Finally, I applied these differentiation systems to two other hiPSC lines. Although the expression levels of various LSEC marker genes were variable in hiPSC lines, hiPSC-derived LSECs highly expressed these marker genes compared with HUVECs (Figure 18). These results demonstrated that inhibition of the TGF β signaling pathway in hypoxic culture promotes the functional maturation of hiPSC-derived LSECs as well as mouse LSECs.

Generation of HSC progenitors from hiPSCs

To produce a large amount of mature HSCs from hiPSCs, I also aimed to generate HSC progenitors capable of proliferation *in vitro*. I demonstrated that ALCAM is a useful cell-surface marker for the isolation of mouse HSC progenitors (Figures 3 and 4A). Therefore, I evaluated the expression of ALCAM in differentiating hiPSCs by FCM analysis. I developed a two-step protocol to generate mature HSCs from hiPSCs (Figure 19). As ALCAM^{high} cells developed after mesoderm differentiation, ALCAM^{high} and ALCAM⁻ cells were sorted by using a cell sorter for further analysis (Figure 20A). ALCAM^{high} cells strongly expressed HSC marker genes such as *DES*, *NGFR*, *CYGB*, and *LRAT* compared with ALCAM⁻ cells (Figure 20B). These results suggested that hiPSC-derived ALCAM^{high} HSC progenitors could be used for the production of mature HSCs.

Maturation of HSCs from hiPSC-derived ALCAM^{high} HSC progenitors

As I had shown that ALCAM^{high} HSC progenitors isolated from mouse fetal livers were proliferative and differentiated following inhibition of the Rho-ROCK signaling pathway (Figures 7 and 8), I sought to compare this result with our hiPSC-derived ALCAM^{high} HSC progenitors, which were cultured in the presence of Y27632 (Figure 19). I found that these cells proliferated (Figure 21A) and exhibited typical mature HSC morphology with projections after 5 days of culture, compared with cells cultured in the absence of Y27632 (Figure 21B). Furthermore, although no significant differences were observed in mRNA expression levels due to variability between experiments, HSC marker genes such as *NGFR*, *LRAT*, and *NES* were markedly increased after treatment with Y27632 (Figure 21C), and the expression levels in hiPSC-derived HSCs treated with Y27632 were much higher than those in human mesenchymal stem cells (MSCs) and primary human HSCs (Figure 22). Conversely, pluripotency and mesodermal marker genes were reduced to undetectable levels after differentiation (Figure 23). hiPSC-derived HSCs also expressed high levels of hepatocyte growth factor (HGF) RNA and protein (Figures 21C and 24), indicating that they may be useful for the generation of functional hepatocytes from hiPSCs. Moreover, because mature HSCs are known to be vitamin A-storing cells, I analyzed this activity in hiPSC-derived HSCs. Vitamin A droplets were observed in hiPSC-derived HSCs (Figure 25A), and FCM analysis of auto-fluorescence from vitamin A by UV irradiation showed that as much as 35% of hiPSC-derived HSCs stored vitamin A (Figure 25B). However, these vitamin A droplets were not detected in human MSCs (Figures 25C and 25D). As expected, those

vitamin A-storing hiPSC-derived HSCs highly expressed HSC marker genes (Figure 25E). These results demonstrated that the Rho-ROCK signaling pathway plays a critical role in the expansion and differentiation of hiPSC-derived ALCAM^{high} HSC progenitors as well as mouse HSCs.

Expansion and maintenance of LPCs in a co-culture system with hiPSC-derived NPCs

Next, I evaluated the ability of hiPSC-derived NPCs (LSECs and HSCs) to support the maintenance of LPCs. hiPSC-derived CPM⁺ LPCs were prepared according to previous protocol (Kido et al., 2015) and cultured on hiPSC-derived NPC feeder cells for 14 days (Figure 26A). CPM⁺ LPCs formed many compact colonies on hiPSC-derived NPC feeder cells, whereas very few colonies were formed on collagen I-coated plates (data not shown) and HUVEC/MSC feeder cells, which we used as a control (Figure 26B). Growth of CPM⁺ LPCs on each feeder cell revealed that CPM⁺ LPCs were highly proliferative on hiPSC-derived NPC feeder cells (Figure 26C). These data indicated that hiPSC-derived NPCs could support proliferation of LPCs. In addition, expression of LPC markers such as *HNF4A*, *AFP*, and *ALB* in CPM⁺ LPCs was dramatically increased by 14 days of culture on hiPSC-derived NPCs (Figure 27A). In this hiPSC-derived liver co-culture system, AFP was also abundantly detected in the culture medium (Figure 27B). Moreover, we investigated whether the expanded CPM⁺ LPCs, simply by co-culture with hiPSC-derived NPCs, maintained their potential for differentiation into hepatocytes. After the induction of hepatic maturation by Oncostatin

M stimulation, hepatocytes from CPM⁺ LPCs showed typical human hepatocyte morphology (Figure 28A) and were positive for ALB and HNF4A (Figure 28B). In addition, these cells produced a large amount of ALB in the culture medium (Figure 28C). Furthermore, they started to express various metabolic enzyme genes such as *PCK1*, *TAT*, *CPS1*, and *G6PC* (Figure 28D). In sharp contrast, the expression of these liver enzymes was not induced in CPM⁺ LPCs cultured on HUVECs/MSCs. These data indicated that expanded LPCs maintained their potential for differentiation into hepatocytes. To induce fully functional hepatocytes from hiPSC-derived LPCs, I also established a high-density co-culture system (Figure 29A). CYP3A4 activity was gradually increased during 10 weeks co-culture (Figure 29B), and hiPSC-derived liver cells expressed some hepatic metabolic enzyme genes at levels comparable with cultured primary human hepatocytes (Figure 29C). I then performed RNA sequencing (RNA-seq) analysis of hiPSC-derived LPCs, hiPSC-derived liver model, and primary human hepatocytes for a more in-depth analysis. Expression of 60 hepatic metabolic enzyme genes was dramatically increased in the hiPSC-derived liver model compared with hiPSC-derived LPCs (Figure 30). Immature hepatocytes or hepatoblasts marker genes such as *AFP*, *EPCAM*, *CD133*, and *DLK1* were still expressed in the hiPSC-derived liver model (data not shown), indicating that there is still a room for improvement on this two-dimensional liver model. Collectively, these results suggest that hiPSC-derived NPCs are able to support proliferation and differentiation of hiPSC-derived LPCs.

Mechanism of hiPSC-derived NPCs in supporting liver development *in vitro*

Finally, I performed microarray analysis to understand how hiPSC-derived NPCs regulate LPC maintenance/differentiation. Among the signaling molecules involved in liver development, I identified 31 genes that showed over 2-fold increase in RNA expression in hiPSC-derived LSECs/HSCs compared with HUVECs/MSCs (Figure 31A). These genes include hepatocyte growth and/or differentiation factors such as HGF, fibroblast growth factors, bone morphogenetic proteins, and midkine as well as extracellular matrices (ECMs) such as collagens and laminins. Microarray results were confirmed by qRT-PCR of the three-independent samples (Figure 31B). Although the contribution of NPCs in human liver development is not completely understood, hiPSC-derived NPCs, especially hiPSC-derived HSCs, might have promoted hepatic maturation of hiPSC-derived LPCs in a high-density co-culture system by secreting these hepatic mitogens and ECMs. Because the interactions between LSECs and HSCs have been considered to contribute to vasculogenesis during liver development *in vivo*, I explored this possibility by microarray and qRT-PCR analysis and showed that hiPSC-derived LSECs and HSCs expressed platelet-derived growth factors (PDGFs)/PDGF receptors and C-X-C chemokine receptor 4 (CXCR4)/CXCL12, which are key molecules for vasculogenesis during liver development (Figures 32). Under the three-dimensional co-culture system of LSECs and HSCs, hiPSC-derived LSECs formed tube-like structures (Figures 33). Additionally, hiPSC-derived LPCs co-cultured with hiPSC-derived NPCs formed compact spheroids compared with hiPSC-derived LPCs without co-culture under the three-dimensional culture system (Figures 34A and

34B). Vessel like structures are formed at the central part of these hiPSC-derived liver spheroids (Figure 34C), suggesting that hiPSC-derived NPCs induced liver organogenesis *in vitro*. Altogether, hiPSC-derived NPCs play important roles for constituting the LPC niche as well as *in vivo* liver development.

Discussion

Characteristics of hiPSC-derived LSECs and HSCs

Studies on liver development have focused mostly on hepatocytes and biliary cells, whereas molecular details of LSEC/HSC differentiation have remained largely unexplored. In this study, I have identified cell surface antigens useful for isolation of LSEC progenitors and HSC progenitors in mouse fetal livers and developed culture systems to expand and differentiate these cells. I found that the TGF β and Rho-ROCK signaling pathway, respectively, regulate the proliferation and maturation of LSECs and HSCs. Based on these results, I have developed efficient and reproducible culture systems to generate LSECs and HSCs from hiPSCs. These hiPSC-derived LSEC progenitors and HSC progenitors could be expanded *in vitro* and exhibited distinct cell-specific characteristics upon induction of maturation. However, characteristics of hiPSC-derived NPCs, especially hiPSC-derived HSCs, were variable between experiments (Figure 21C). To produce homogeneous HSCs from hiPSCs, it is required to isolate the homogeneous HSC progenitor population by combining other cell surface antigens with ALCAM.

Primary non-parenchymal cells appear to rapidly lose their functions because the expression levels of LSEC- and HSC-specific markers in commercially available primary cells were variable and much lower than hiPSC-derived LSECs and HSCs. Thus, my culture systems provide a means to make LSECs and HSCs with much better

functions.

Tissue-specific endothelial cells and mesenchymal cells

hiPSC-derived NPCs highly expressed several hepatic mitogens and ECMs and supported self-renewal of hiPSC-derived LPCs in the two-dimensional culture system without the need for exogenous cytokines. CPM⁺ LPCs expanded on hiPSC-derived NPCs can be induced to express various hepatic genes. In contrast, neither proliferation nor differentiation of LPCs was supported by HUVECs and MSCs, which were derived from umbilical cord and bone marrow, respectively. Recently, ‘organ bud technology’ has been developed using hiPSC-derived endodermal cells (liver progenitor cells) mixed with HUVECs and MSCs. (Takebe et al., 2013). They showed that hiPSC-derived liver buds do not exhibit liver functions *in vitro* but become functional after transplantation in mice. These results indicate that tissue-specific endothelial cells and mesenchymal cells are necessary for the generation of functional tissue *in vitro*. hiPSC-derived LSECs exhibited distinctive phenotypes of LSECs because these cells expressed *FCGR2B*, *STAB2*, and *F8*, that expressed in LSECs, not in other endothelial cells such as arterial and venous endothelial cells. hiPSC-derived HSCs also exhibited cell-specific phenotypes of HSCs because these cells have a vitamin-A storage activity. Therefore, hiPSC-derived LSECs and HSCs are liver specific endothelial and mesenchymal cells, and are ideal cells for generating mature liver tissue *in vitro*.

Three-dimensional human liver co-culture models

Three-dimensional culture has been reported to promote the hepatic maturation than two-dimensional culture (Ogawa et al., 2013; Takayama et al., 2013). Moreover, hepatoblasts differentiate into mature hepatocytes through interactions with non-parenchymal cells (NPCs) during liver development *in vivo* under the three-dimensional environment. After induction of hepatic maturation by two-dimensional co-culture of hiPSC-derived LPCs with NPCs, the hiPSC-derived liver model still exhibited immature phenotypes with limited function compared with primary human hepatocytes (Figure 30). In order to induce fully functional hepatocytes from hiPSCs, it is essential to develop a three-dimensional co-culture system by mimicking human liver development using hiPSC-derived LPCs, LSECs, and HSCs. Three-dimensional bioprinting techniques and cell sheet engineering would be useful for mimicking liver development and constructing liver structure *in vitro*.

I have clearly shown that iPSC-derived HSCs, but not iPSC-derived LSECs, play an important role for hepatic maturation by producing a number of hepatic mitogens and extracellular matrix proteins. During liver development *in vivo*, the interactions between LSECs and HSCs have been considered to contribute to vasculogenesis. In my study, hiPSC-derived LSECs and HSCs highly expressed key molecules for vasculogenesis, and hiPSC-derived LSECs formed tube-like structures under the three-dimensional culture. Therefore, it is supposed that hiPSC-derived LSECs organize the liver microvasculature by interaction with hiPSC-derived HSCs in three-dimensional

co-culture system.

Application of hiPSC-derived liver cells

As the liver consists primarily of hepatocytes, they are the major target cells in various liver diseases such as viral hepatitis, alcoholic liver disease, and nonalcoholic fatty liver disease. NPCs also involve in some liver diseases, and play an important role in liver regeneration through direct and/or indirect pathways (Giugliano S et al., 2015; Friedman SL., 2000; DeLeve LD., 2013). Liver fibrosis is induced in various liver injuries and leads to cirrhosis and liver cancer, a leading cause of death. Because activated HSCs in response to inflammatory reactions of hepatic disorder produce extracellular matrix such as various types of collagen, these cells are known to be a key regulator of liver fibrosis (Friedman SL., 2000). Therefore, in order to develop new therapeutic approach for this disease, it is important to recapitulate the HSC activation process *in vitro*. However, HSCs isolated from livers exhibited activated phenotypes in culture (de Leeuw AM et al., 1984), and hiPSC-derived HSCs expressed activated HSC marker genes such as *ACTA2* and *COL1A1* (data not shown). Therefore, it is necessary to develop a novel differentiation culture system for quiescent HSCs from hiPSCs by modifying the original culture system in this study. Additionally, as interactions between hepatocytes, LSECs, and HSCs are important for progression of liver fibrosis *in vivo*, it would be necessary to develop a multi cellular liver fibrosis model to reproduce the progression of liver fibrosis *in vitro*.

On the other hands, LSECs are considered to play a role for hemostasis by producing coagulation factor, Factor VIII (F8). The inactivation of this gene causes hemophilia A. Until now, although prophylactic replacement therapy with recombinant or plasma derived factor VIII was major treatment for hemophilia A, this treatment requires frequent administration, a heavy burden on the patients. Because hiPSC-derived LSECs highly express Factor VIII, hiPSC-derived LSECs may be useful for cell-based therapy for hemophilia A.

Consequently, because various mature liver functions are reproduced *in vitro* by co-culture of parenchymal hepatocytes with non-parenchymal cells, the hiPSC-derived the human liver model will be useful for disease modeling, drug screening, and cell therapy.

Conclusion

In the present study, I showed that LSEC progenitors and HSC progenitors in mouse fetal livers can be isolated based on expression of their specific cell-surface markers and developed culture systems to expand and differentiate these cells to their mature stages. I found that the TGF β and Rho-ROCK signaling pathway, respectively, regulate the proliferation and maturation of LSECs and HSCs isolated from mouse fetal livers (Figure 9). Based on these observations in mice, I have established efficient culture systems to generate LSECs and HSCs from human iPS cells. hiPSC-derived LSECs and HSCs exhibited their distinct cell-type specific characteristics, respectively. Additionally, these hiPSC-derived NPCs highly expressed various hepatic mitogens and ECMs and supported the proliferation and differentiation of hiPSC-derived LPCs (Figure 35). The hiPSC-derived liver model expressed some hepatic metabolic enzyme genes at levels comparable to those cultured primary human hepatocytes. Thus, hiPSC-derived LPCs and NPCs are useful for developing a functional human liver model *in vitro*, which will be useful for drug screening, pathological models, and cell therapy.

References

Asahina, K., Tsai, S.Y., Li, P., Ishii, M., Maxson, R.E. Jr., Sucov, H.M., and Tsukamoto, H. (2009). Mesenchymal origin of hepatic stellate cells, submesothelial cells, and perivascular mesenchymal cells during mouse liver development. *Hepatology* 49, 998-1011.

Asahina, K., Zhou, B., Pu, W.T., and Tsukamoto, H. (2011). Septum transversum-derived mesothelium gives rise to hepatic stellate cells and perivascular mesenchymal cells in developing mouse liver. *Hepatology* 53, 983-995.

de Leeuw, A.M., McCarthy, S.P., Geerts, A., Knook, D.L. (1984). Purified rat liver fat-storing cells in culture divide and contain collagen. *Hepatology* 4, 392-403.

DeLeve, L.D. (2013). Liver sinusoidal endothelial cells and liver regeneration. *J Clin Invest* 123, 1861-1866.

Friedman, S.L. (2000). Molecular regulation of hepatic fibrosis, an integrated cellular response to tissue injury. *J Biol Chem* 275, 2247-2250.

Giugliano, S., Kriss, M., Golden-Mason, L., Dobrinskikh, E., Stone, A.E., Soto-Gutierrez, A., Mitchell, A., Khetani, S.R., Yamane, D., Stoddard, M., et al (2015). Hepatitis C virus infection induces autocrine interferon signaling by human liver endothelial cells and release of exosomes, which inhibits viral replication. *Gastroenterology* 148, 392-402.

Hentsch, B., Lyons, I., Li, R., Hartley, L., Lints, T.J., Adams, J.M., and Harvey, R.P. (1996). Hlx homeo box gene is essential for an inductive tissue interaction that drives

expansion of embryonic liver and gut. *Genes Dev* 10, 70-79.

Kattman, S.J., Witty, A.D., Gagliardi, M., Dubois, N.C., Niapour, M., Hotta, A., Ellis, J., and Keller, G. (2011). Stage-specific optimization of activin/nodal and BMP signaling promotes cardiac differentiation of mouse and human pluripotent stem cell lines. *Cell Stem Cell* 8, 228-240.

Kido, T., Kouji, Y., Suzuki, K., Kobayashi, A., Miura, Y., Chern, E.Y., Tanaka, M., and Miyajima, A. (2015). CPM Is a Useful Cell Surface Marker to Isolate Expandable Bi-Potential Liver Progenitor Cells Derived from Human iPS Cells. *Stem Cell Reports* 5, 508-515.

Matsumoto, K., Yoshitomi, H., Rossant, J., and Zaret, K.S. (2001). Liver organogenesis promoted by endothelial cells prior to vascular function. *Science* 294: 559-563.

Murata, T., Arii, S., Nakamura, T., Mori, A., Kaido, T., Furuyama, H., Furumoto, K., Nakao, T., Isobe, N., and Imamura, M. (2001). Inhibitory effect of Y-27632, a ROCK inhibitor, on progression of rat liver fibrosis in association with inactivation of hepatic stellate cells. *J Hepatol* 35, 474-481.

Nonaka, H., Tanaka, M., Suzuki, K., and Miyajima, A. (2007). Development of murine hepatic sinusoidal endothelial cells characterized by the expression of hyaluronan receptors. *Dev Dyn* 236, 2258-2267.

Nonaka, H., Watabe, T., Saito, S., Miyazono, K., and Miyajima, A. (2008). Development of stabilin2⁺ endothelial cells from mouse embryonic stem cells by inhibition of TGFβ/activin signaling. *Biochem Biophys Res Commun* 375, 256-260.

Ogawa, S., Surapisitchat, J., Virtanen, C., Ogawa, M., Niapour, M., Sugamori, K.S.,

Wang, S., Tambllyn, L., Guillemette, C., Hoffmann, E., et al. (2013). Three-dimensional culture and cAMP signaling promote the maturation of human pluripotent stem cell-derived hepatocytes. *Development* 140, 3285-3296.

Okita, K., Matsumura, Y., Sato, Y., Okada, A., Morizane, A., Okamoto, S., Hong, H., Nakagawa, M., Tanabe, K., Tezuka, K., et al. (2011). A more efficient method to generate integration-free human iPS cells. *Nat Methods* 8, 409-412.

Onitsuka, I., Tanaka, M., Miyajima, A. (2010). Characterization and functional analyses of hepatic mesothelial cells in mouse liver development. *Gastroenterology* 138, 1525-1535.

Shinohara, M., Komori, K., Fujii, T., Sakai, Y. (2017). Enhanced self-organization of size-controlled hepatocyte aggregates on oxygen permeable honeycomb microwell sheets. *Biomed. Phys. Eng. Express* 3, 045017.

Si-Tayeb, K., Noto, F.K., Nagaoka, M., Li, J., Battle, M.A., Duris, C., North, P.E., Dalton, S., and Duncan, S.A. (2010). Highly efficient generation of human hepatocyte-like cells from induced pluripotent stem cells. *Hepatology* 51, 297-305.

Takahashi, K., Tanabe, K., Ohnuki, M., Narita, M., Ichisaka, T., Tomoda, K., Yamanaka, S. (2007) Induction of pluripotent stem cells from adult human fibroblasts by defined factors. *Cell* 131, 861-872.

Takayama, K., Inamura, M., Kawabata, K., Sugawara, M., Kikuchi, K., Higuchi, M., Nagamoto, Y., Watanabe, H., Tashiro, K., Sakurai, F., et al. (2012). Generation of metabolically functioning hepatocytes from human pluripotent stem cells by FOXA2 and HNF1a transduction. *J. Hepatol.* 57, 628-636.

Takayama, K., Kawabata, K., Nagamoto, Y., Kishimoto, K., Tashiro, K., Sakurai, F., Tachibana, M., Kanda, K., Hayakawa, T., Furue, M.K., Mizuguchi, H. (2013). 3D spheroid culture of hESC/hiPSC-derived hepatocyte-like cells for drug toxicity testing. *Biomaterials* 34, 1781-1789

Takayama, N., Nishimura, S., Nakamura, S., Shimizu, T., Ohnishi, R., Endo, H., Yamaguchi, T., Otsu, M., Nishimura, K., Nakanishi, M., et al. (2010). Transient activation of c-MYC expression is critical for efficient platelet generation from human induced pluripotent stem cells. *J Exp Med* 207, 2817-2830.

Takebe, T., Sekine, K., Enomura, M., Koike, H., Kimura, M., Ogaeri, T., Zhang, R.R., Ueno, Y., Zheng, Y.W., Koike, N., et al. (2013). Vascularized and functional human liver from an iPSC-derived organ bud transplant. *Nature* 499, 481-484.

Tanaka, M., Okabe, M., Suzuki, K., Kamiya, Y., Tsukahara, Y., Saito, S., and Miyajima, A. (2007). Mouse hepatoblasts at distinct developmental stages are characterized by expression of EpCAM and DLK1: drastic change of EpCAM expression during liver development. *Mech Dev* 126, 665-676.

Tremblay, K.D., and Zaret, K.S. (2005). Distinct populations of endoderm cells converge to generate the embryonic liver bud and ventral foregut tissues. *Dev. Biol.* 280, 87-99.

White, M.P., Rufaihah, A.J., Liu, L., Ghebremariam, Y.T., Ivey, K.N., Cooke, J.P., and Srivastava, D. (2013). Limited gene expression variation in human embryonic stem cell and induced pluripotent stem cell-derived endothelial cells. *Stem Cells* 31, 92-103.

Yin, C., Evason, K.J., Asahina, K., Stainier, D.Y. (2013). Hepatic stellate cells in liver

development, regeneration, and cancer. *J Clin Invest* 123, 1902-1910.

Figures and Tables

Table 1. List of primary and secondary antibody used for immunocytochemistry analysis and FCM analysis of human cells

Primary Antibody	Supplier
Stabilin2	Nonaka et al.
CD31	NeoMarkers (RB-10333-P0)
CD31-PE	BD Bioscience (555446)
CD34-FITC	BioLegend (343604)
CD309(FLK1)-APC	Miltenyi Biotec (130-093-601)
CD32(Fc γ RII)-APC	BioLegend (303208)
CD166(ALCAM)-biotin	Miltenyi Biotec (130-106-574)
F8	abcam (ab41187)
ALB	Nippon bio-test laboratories (0902-1)
HNF4 α	SantaCruz (sc-6556)

Secondary Antibody	Supplier
Streptavidin-APC	BD Bioscience (554067)
Alexa Fluor 488 anti-Rat IgG	Life Technologies (A21208)
Alexa Fluor 488 anti-Mouse IgG	Life Technologies (A21202)
Alexa Fluor 555 anti-Mouse IgG	Life Technologies (A21424)
Alexa Fluor 555 anti-Goat IgG	Life Technologies (A21432)
Alexa Fluor 647 anti-Mouse IgG	Life Technologies (A31571)

Table 2. List of Chemicals, recombinant proteins, mediums, and peptides for cell culture experiments

Reagent	Source
GFR matrigel	Corning
fetal bovine serum	JRH Biosciences
bFGF	Life Technologies
BMP4	Life Technologies
fibronectin	Life Technologies
insulin-transferrin-selenium	Life Technologies
L-glutamine	Life Technologies
MEM non-essential amino acids	Life Technologies
N2 supplement	Life Technologies
penicillin-streptomycin-glutamine	Life Technologies
Stempro-34 SFM	Life Technologies
EGM-2	Lonza
HCM	Lonza
MSCGM	Lonza
collagen Type I-A	Nitta Gelatin
collagen Type I-C	Nitta Gelatin
Activin A	PeproTech
EGF	PeproTech
HGF	PeproTech
oncostatin M	PeproTech
VEGF	PeproTech
ascorbic acid	Sigma-Aldrich
DMEM/F12	Sigma-Aldrich
N-acetylcysteine	Sigma-Aldrich
nicotinamide	Sigma-Aldrich
Retinol	Sigma-Aldrich
A83-01	Tocris
Dorsomolpin	Tocris
SB431542	Tocris
Y27632	Wako Pure Chemical Industries, Ltd.
dexamethasone	Wako Pure Chemical Industries, Ltd.

Table 3. List of Quantitative PCR primers for mouse and human genes

		Left Primer	Right Primer
Mouse	<i>Actb</i>	TTCTTTGCAGCTCTTCGTT	ATGGAGGGGAATACAGCCC
	<i>Stab2</i>	TGTCAGACGGCTACATCAA	CCAGGGATATCCAGGACGTA
	<i>Lyve1</i>	CCTCCAGCCAAAAGTTCAAA	TCCAACACGGGGTAAAATGT
	<i>F8</i>	TCATGTATAGCTGGATGGGA	GATGAGTCCACATTGCCAAA
	<i>CD34</i>	TGGGTAGCTCTGCTGTAT	TGGTAGGAACTGATGGGGAT
	<i>CD31</i>	CTGGTGTCTATGCAAGCCT	AGTTGTGCCCATTCATCAC
	<i>Des</i>	GTGAAGATGGCCTTGGATGT	CTCGGAAGTTGAGAGCAGAGA
	<i>Ngfr</i>	GTGTGCGAGGACACTGAGC	GGGGGTAGACCTTGTGATCC
	<i>Cygb</i>	GCTGTATGCCAAGTGCAG	CCTCCATGTCTAAACTGGC
	<i>Lrat</i>	TATGGCTCTCGGATCAGTCC	CTAATCCCAAGACAGCCGAA
	<i>Hgf</i>	CCTGACACCACTGGGAGTA	CTTCTCCTGGCCTTGAATG
	<i>HNF4a</i>	TTAAGAAGTGTTCGGGCT	GCTGTCTCGTAGCTTGACC
	<i>AFP</i>	GGCGATGGGTTTAGAAAAG	CAGCAGCCTGAGATCCATA
	<i>Alb</i>	TGCACACTCCAGAGAAGGA	GTCTCAGTTGCTCCGCTGT
	Human	<i>ACTB</i>	GCACAGAGCTTCGCCTT
<i>OCT4</i>		GAAGGAGAAGCTGGAGCAAA	CTTCTGCTTCAGGAGCTTGG
<i>MESP1</i>		GATGGAGCCAAGCCAC	CTCAGGACGCCACTCCAG
<i>CD31</i>		AGGCCCAATACACTCACA	CGGGGAATCCAGATACAC
<i>VE-Cad</i>		TGGAGAAGTGGCACTCAGCAACA	TCTACATCCCTTGCAGTGTGAG
<i>STAB2</i>		CCTGTGAAACCTGTGCTGAC	CCATCCCAATCTTCCACTG
<i>LYVE1</i>		ACTTCCATCTGGACCA	CCTTTTGTCCACAAG
<i>FLT4</i>		CTCTGCCTGGGACTCCTG	GGTGTGATGACGCTGTGACT
<i>FLK1</i>		CCTGTATGGAGGAGGAGGAA	CGGCTCTTCGCTTACTGTT
<i>CD34</i>		GCCATTGAGCAAGCAACAC	AAGGGTTGGGCGTAAGAGAT
<i>FcγRIIB</i>		AGCCTTGGGGTCAATAGCTT	AGTTTCAGCACAGCCTTTGG
<i>F8</i>		CTTTTGCATCTGCTTAGTGC	TAGGAGGAAATCTGCGTCCA
<i>ALCAM</i>		CTTCTGCCTCTTGATCTCCG	AGGTACGCTCAAGTCGGCAAG
<i>DES</i>		GAAGCTGCTGGAGGGAGAG	ATGGACCTCAGAACCCCTTT
<i>NGFR</i>		CTGTGCTGTGTGCTTCT	CAGGCTTGCAGCCTCAC
<i>CYGB</i>		TCTATGCCAAGTGCAGGAC	TCCTCCATGTCTTGAAGT
<i>LRAT</i>		TACTGCAGATATGGCACCC	CCAAGACTGCTGAAGCAAGA
<i>NES</i>		AAGATGTCCTCAGCTGG	GAGGGAAGTCTGGAGCCAC
<i>HGF</i>		CGCTGGGAGTACTGTGCAAT	CCCTGTAGCCTTCTCTTGA
<i>NANOG</i>		GATTTGTGGGCTGAAGAAA	ATGGAGGAGGGGAAGAGGAGA
<i>T</i>		AATTGGTCCAGCCTTGAA	TGCTCACAGACCACAGGC
<i>HNF4a</i>		GCAGGCTCAAGAAA TGCTTC	GGCTGTCTCCTCATAGCTT
<i>AFP</i>		AGAGGAGATGTGCTGGA TTG	GTGGTCAGTTTGCAGCA TTC
<i>ALB</i>		TGCTGA TGAGTACGCTGAAAA	TCAGCCATTCACCATAGGTT
<i>PCK1</i>		GAGAAAAGCTTCAATGCCAG	ATGCCGATCTTTGACAGAGG
<i>TAT</i>		ATAATGGCTATGCCCATCC	CCTTAGCTTCTAGGGGTGCC
<i>CPS1</i>		GGAAAAGACACTGAAAGGGCT	CCCAAGGCATTTGAAATCT
<i>G6PC</i>		CTACAGCAACTTCCGTGC	GTATACACTGTGTGCCCAT
<i>CYP3A4</i>		TTTTGTCTTACCATAAGGGCTTT	CACAGGCTGTTGACCATCAT
<i>CYP2C19</i>		TTGCTTCTGATCAAAATGG	GTCTCTGTCCAGCTCCAAG
<i>CYP1A2</i>		CTTCGTAAACCAAGTGGCAGG	AGGGCTTGTAAATGGCAGTG
<i>FGF9</i>		GTGGACTTACCTCGGATG	CCAGTTTCTTCGAAGTGTCTC
<i>FGF10</i>		TGCTGTTAATGGCTTTGACG	AGAAGAACGGGAAGGTCAGC
<i>FGF13</i>		GTCTGCGAGTGGTGGCTATC	TGAATTTGCACTCAGGTGTGA
<i>FGF18</i>		ACTTCTGCTGCTGTGCTTC	CTTACGGCTCACATCGTCC
<i>FGF20</i>		GCTTCCACCTGCAGATCCT	GCCACACTGATGAATCCAA
<i>BMP2</i>		CACTGTGGCAGCTTCC	CCTCCGTGGGATAGAACTT
<i>BMP5</i>		TAGCCAGCTCCATGATACC	TTCCGTGTTGAGAAAATCC
<i>BMP7</i>		TGGTCAATGAGCTTCGTCAAC	TGGAAAAGATCAAAACCGAAC
<i>BMP10</i>		CAAAATTTGCAACAGATCGGA	TTCCGGAGCCATAAAAATG
<i>IGF1</i>		TGGAATGCTTCTCAGTTCGTG	TCATCCACGATGCTGTCT
<i>IGF2</i>		GTTCGGTTTGCACACG	AGAAGCACAGCATCGACTT
<i>MDK</i>		GTCCCGGGTTATACAG	GAGGTGAGCCAGCAG
<i>LAMA1</i>		CCTGGTCTGTGCTGTGT	TTGGTGTGATGTGAGCATT
<i>LAMA5</i>		GCTGGTGGCAGAGTCCAC	GGCAAACTGTATGAGGACGTA
<i>LAMC3</i>		CCACCTCGGTCAACATCAC	CGCTGTAGATGGCAAAGC
<i>COL2A1</i>		CTGTCTTCGGTGTACGGG	CGGCTTCCACACATCCTTAT
<i>COL3A1</i>		AGGGGAGCTGGCTACTTCTC	AGGACTGACCAAGATGGGAA
<i>COL4A1</i>		CTCCACGAGGAGCACAGC	CCTTTTGTCCCTTCACTCCA
<i>COL4A4</i>		TGTTTCTGAAAAGGGGTC	CCTTTCTCTCTGAAAGCCC
<i>COL4A5</i>		TACTGGCCCTGAGTCTTTGG	TTTCCCTTTTATGCCACTG
<i>COL4A6</i>		CTGCTCCTGGTTACGTTGTG	GGAAAACACTGACAGCTCCC
<i>COL6A6</i>		TCTATGGCCGATGTTGTTC	CTTCCAGTTCGGGGAGAA
<i>COL9A2</i>		GTGAGGAAGTCTAGGGGA	CCTTTCGGGCTGTGAT
<i>COL9A3</i>		AAGGGAGACCAGGGTATTGC	TCGACTGCCAGACTCTCCTT
<i>COL11A1</i>		AATGGAATCACGGTTTTTGG	GTCAATGCTGCCTTGGGAT
<i>COL15A1</i>		CAGTGTGTTGTCTGCTGAT	CCTGGGAAGCAGTCTCTGTC
<i>COL19A1</i>	AGGCAGCAAAGGAGAAAAGT	GGACCCAAGTCACTTTCAA	
<i>COL21A1</i>	CCCGAGCTGGACACTG	GAAGAAGCAGCACAAAACC	
<i>COL23A1</i>	GAAGTCCATCCGAATGTGT	GGTAGCCATCTGCTCTGAT	
<i>COL25A1</i>	GAATCGCAAGAGAAGCACCT	TGTCAGGAGGACCAGATTTC	
<i>CXCR4</i>	AGGAAGCTGTTGGCTGAAAA	CTCACTGACGTTGGCAAAGA	
<i>CXCL12</i>	TTGACCCGAAGTAAAGTGG	TGGGCTCTACTGTAAGGGTT	
<i>PDGFB</i>	CTGGCATGCAAGTGTGAGAC	AATGGTACCCGAGTTTGG	
<i>PDGFRB</i>	AACTGTGCCACACCAGAAG	CAGGAGAGACAGCAACAGCA	

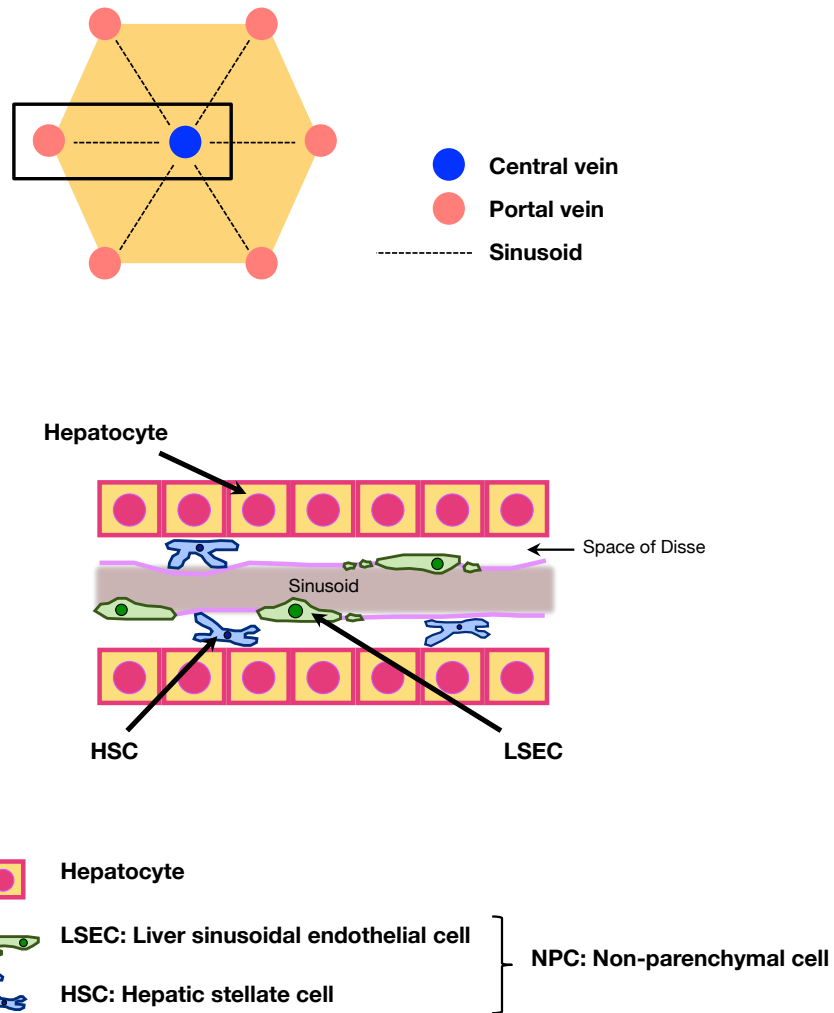


Figure 1. Structure of the liver

The liver is organized into lobules, functional and structural units of the liver. LSECs compose the wall of sinusoids between the central vein and portal vein. HSCs reside in a space of Disse between hepatocytes and LSECs.

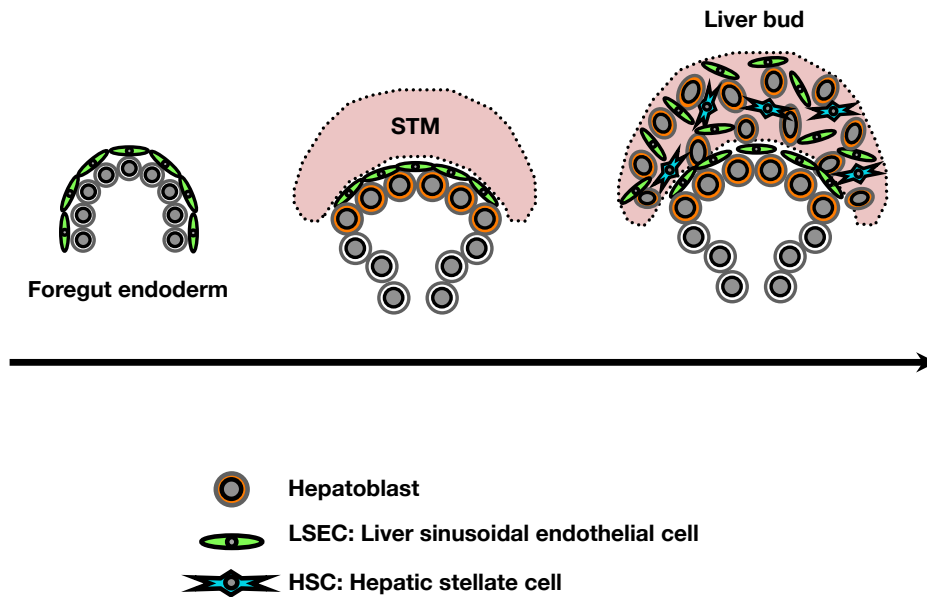


Figure 2. Liver development in mice

Liver development starts with the hepatic specification of the foregut endoderm. Hepatoblasts derived from endoderm cells migrate into the septum transversum mesenchyme (STM) to form the liver bud. Hepatic maturation is induced through interactions with hepatic non-parenchymal cells (NPCs) such as liver sinusoidal endothelial cells (LSECs) and hepatic stellate cells (HSCs).

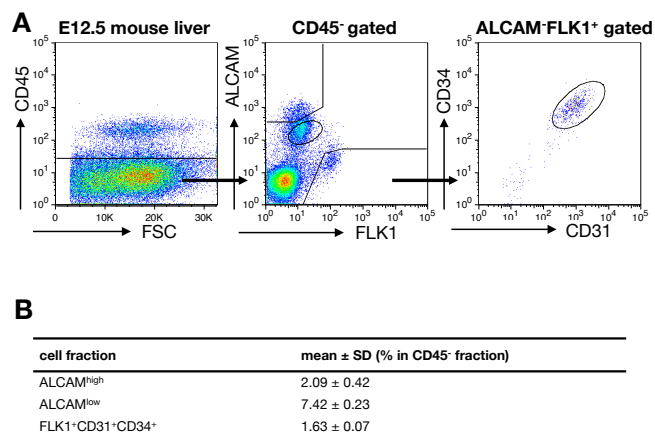


Figure 3. Identification of fetal mouse LSEC, HSC progenitors

(A) FCM analysis of fetal mouse liver cells at E12.5. CD45-FLK1⁺ cells, CD45-ALCAM^{high} cells, and CD45-ALCAM^{low} cells were identified (middle). CD45-FLK1⁺ cells also expressed CD31 and CD34 (right). Positive gates were defined by the isotype control.

(B) Percentages of each cell population are shown as the mean \pm SD of 3 independent experiments.

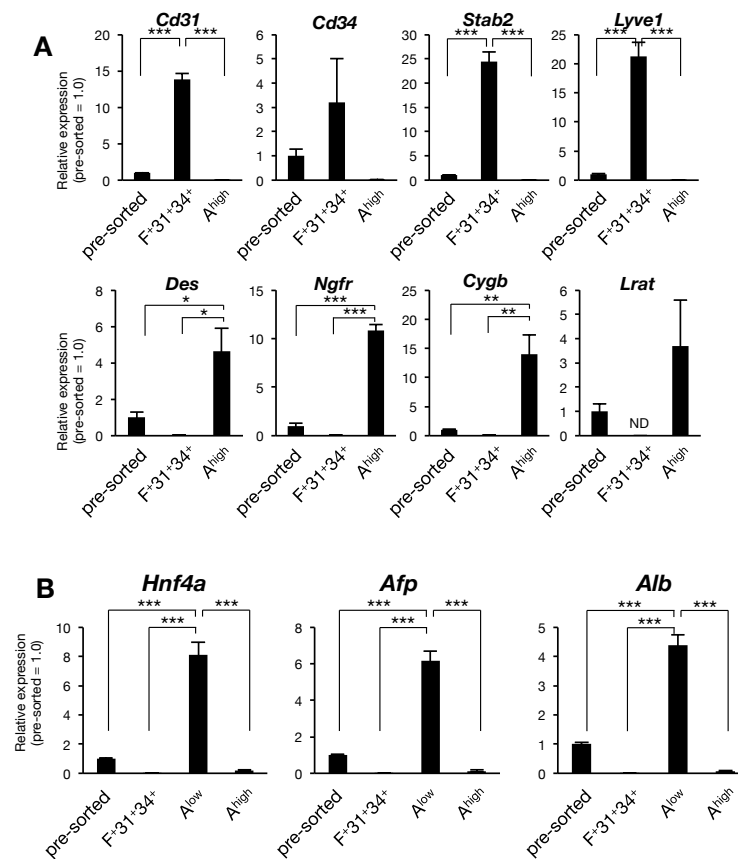


Figure 4. Gene expression of cell type specific markers in fetal mouse livers

(A) qRT-PCR analysis of LSEC progenitor and HSC progenitor marker genes in pre-sorted cells (pre-sorted), CD45-FLK1⁺CD31⁺CD34⁺ cells (F⁺31⁺34⁺), and CD45-ALCAM^{high} cells (A^{high}). n = 3 in each group (each experiment contains 2 technical replicates). The results are shown as the mean ± SEM. *p < 0.05, **p < 0.01, ***p < 0.001.

(B) qRT-PCR analysis of LPC marker genes in pre-sorted cells (pre-sorted), CD45-FLK1⁺CD31⁺CD34⁺ cells (F⁺31⁺34⁺), CD45-ALCAM^{low} cells (A^{low}), and CD45-ALCAM^{high} cells (A^{high}). n = 3 in each group (each experiment contains 2 technical replicates). The results are shown as the mean ± SEM. ***p < 0.001.

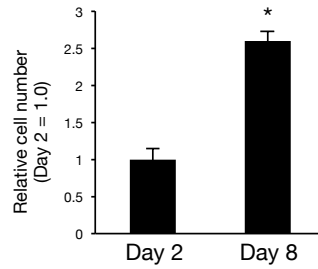


Figure 5. Growth of LSEC progenitors isolated from fetal mouse livers

Relative cell numbers of CD45⁻FLK1⁺CD31⁺CD34⁺ LSEC progenitors isolated from the fetal mouse liver after 2 days and 8 days of culture. n = 3 in each group. The results are shown as the mean \pm SEM. *p < 0.05.

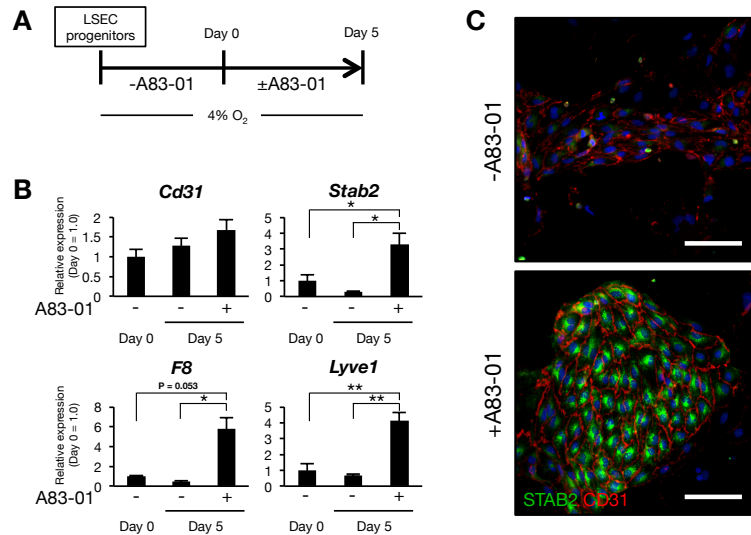


Figure 6. The effect of A83-01 treatment on induction of LSEC differentiation

(A) Schematic representation of the culture system for mouse LSEC progenitors.

(B) Expression levels of the endothelial marker (*Cd31*) and LSEC-specific markers (*Stab2*, *F8*, and *Lyve1*) in CD45-FLK1⁺CD31⁺CD34⁺ LSEC progenitors with or without A83-01 treatment (day 5). CD45-FLK1⁺CD31⁺CD34⁺ LSEC progenitors were used as a control (day 0). The results are shown as the mean ± SEM of 3 independent experiments (each experiment contains 2 technical replicates). *p < 0.05, **p < 0.01.

(C) Immunofluorescence staining for LSEC markers in CD45-FLK1⁺CD31⁺CD34⁺ LSEC progenitors after 5 days of culture with or without A83-01 treatment. STAB2 (green) and CD31 (red). Nuclei were counterstained with Hoechst 33342 (blue). Scale bars, 100 μm.

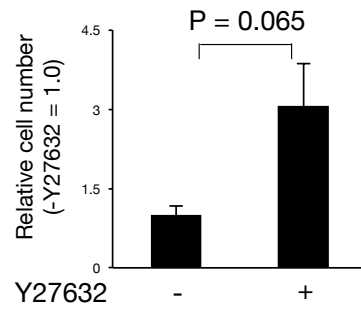


Figure 7. Growth of HSC progenitors isolated from fetal mouse livers

Growth of CD45-ALCAM^{high} HSC progenitors with or without Y27632 treatment for 5 days culture. The results are shown as the mean ± SEM of 3 independent experiments.

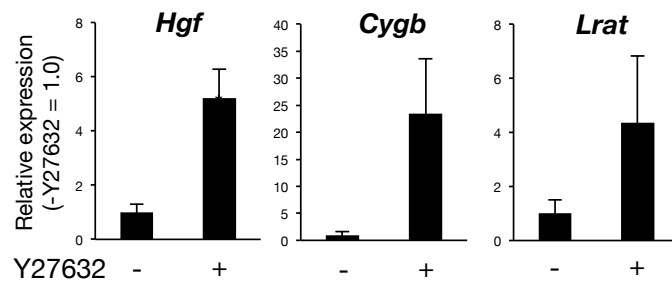


Figure 8. The effect of Y27632 treatment on induction of HSC differentiation

Expression levels of the HSC markers in CD45⁻ALCAM^{high} HSC progenitor cells with or without Y27632 treatment for 5 days. The results are shown as the mean ± SEM of 3 independent experiments (each experiment contains 2 technical replicates). *p < 0.05.

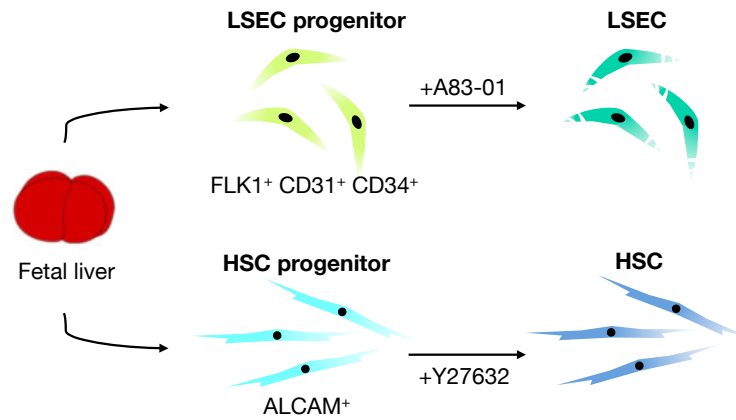


Figure 9. Summary of the mouse study

FLK1, CD31, and CD34 are specific cell-surface markers to enrich LSEC progenitors. ALCAM is a cell-surface marker of HSC progenitors. TGF β and Rho-ROCK signaling pathway, respectively, regulated proliferation and maturation of LSEC and HSC progenitors isolated from fetal mouse livers.

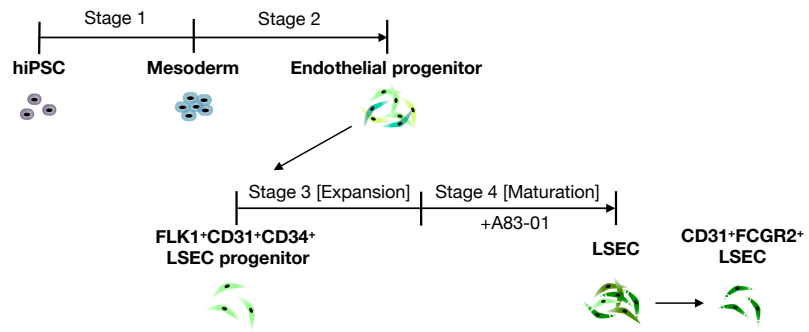


Figure 10. LSEC differentiation from hiPSCs

Schematic representation of LSEC differentiation from hiPSCs.

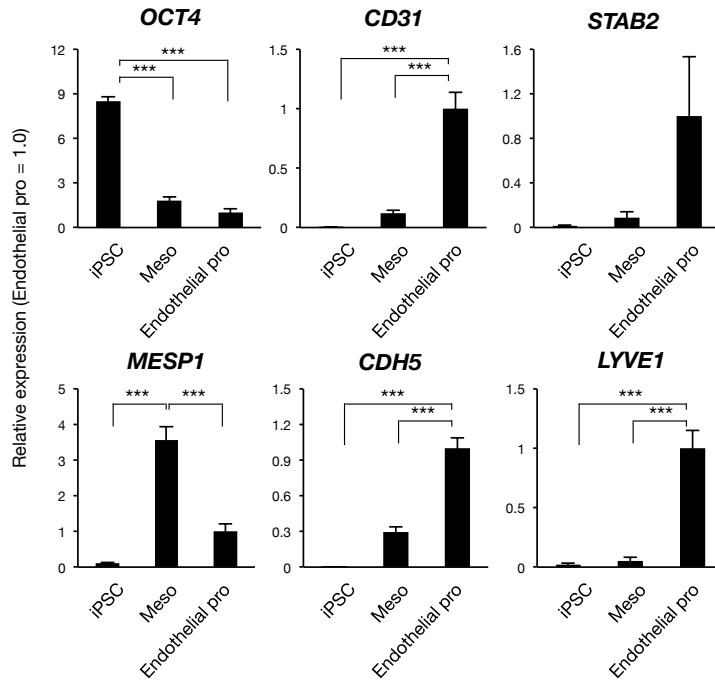


Figure 11. Gene expression of stage specific markers during LSEC differentiation

Expression levels of pluripotent marker gene (*OCT4*), mesodermal cell marker gene (*MESP1*), endothelial cell marker genes (*CD31* and *CDH5*), and LSEC marker genes (*STAB2* and *LYVE1*) in hiPSCs (iPSC), hiPSC-derived mesodermal cells without purification (Meso) and hiPSC-derived endothelial progenitors without purification (Endothelial pro). The results are shown as the mean \pm SEM of independent experiments (each experiment contains 2 technical replicates). n = 3, 5, 5 in each group. ***p < 0.001.

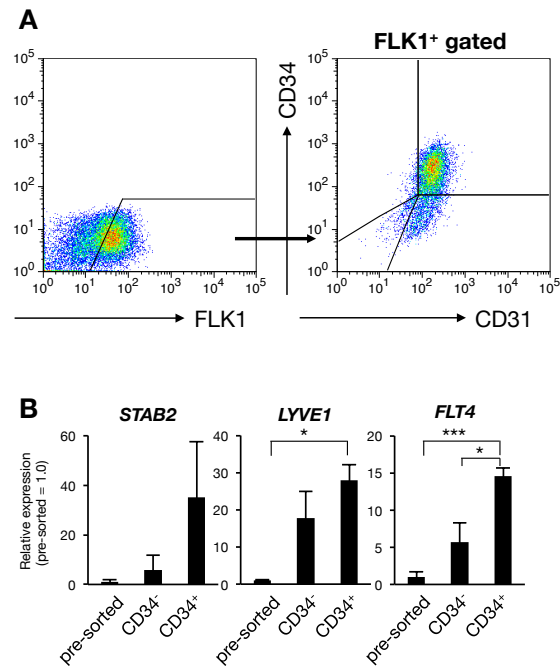


Figure 12. Isolation of hiPSC-derived LSEC progenitors

(A) FCM analysis of hiPSC-derived endothelial progenitor stage. FLK1⁺ cells were identified (left), and CD31⁺CD34^{+/-} cells were identified in FLK1⁺ cell fraction (right).

(B) Expression levels of LSEC-specific marker genes in hiPSC-derived FLK1⁺CD31⁺CD34⁺ cells (CD34⁺) compared with FLK1⁺CD31⁺ CD34⁻ cells (CD34⁻) and pre-sorted cells (pre-sorted). The results are shown as the mean ± SEM of 3 independent experiments (each experiment contains 2 technical replicates). *p < 0.05, ***p < 0.001.

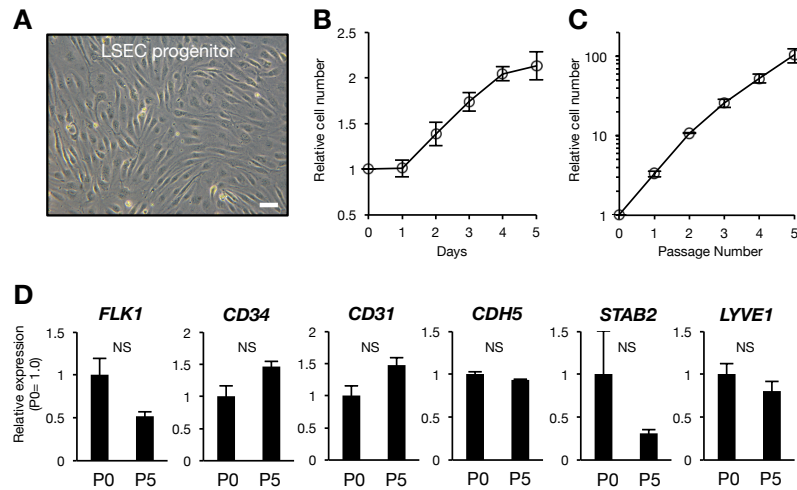


Figure 13. Characteristics of hiPSC-derived FLK1⁺CD31⁺CD34⁺ LSEC progenitor cells

(A) Phase contrast image of FLK1⁺CD31⁺CD34⁺ LSEC progenitor cells after expansion. Scale bar, 100 μ m.

(B) Growth curve of FLK1⁺CD31⁺CD34⁺ LSEC progenitor cells. Each value was determined 3 independent experiments and shown as the mean \pm SEM.

(C) Relative cell numbers of FLK1⁺CD31⁺CD34⁺ LSEC progenitor cells after several passages. Each value was determined from 3 independent experiments and shown as the mean \pm SEM.

(D) Expression of LSEC progenitor cell markers in FLK1⁺CD31⁺CD34⁺ LSEC progenitor cells after 5 times passages. P0: passage 0, P5: passage 5. NS: no significance. The results are shown as the mean \pm SEM of 3 independent experiments (each experiment contains 2 technical replicates).

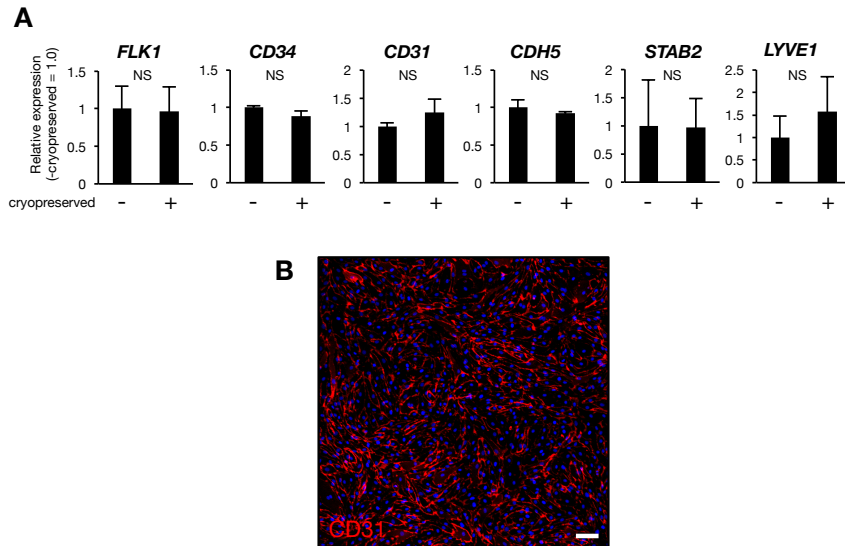


Figure 14. Cryopreservation of hiPSC-derived FLK1⁺CD31⁺CD34⁺ LSEC progenitor cells

(A) Expression of LSEC progenitor cell markers in FLK1⁺CD31⁺CD34⁺ LSEC progenitor cells after cryopreservation. NS: no significance. The results are shown as the mean \pm SEM of 3 independent experiments (each experiment contains 2 technical replicates).

(B) Immunofluorescence analysis for CD31 (red) in FLK1⁺CD31⁺CD34⁺ LSEC progenitor cells after cryopreservation. Nuclei were counterstained with Hoechst 33342 (blue). Scale bars, 100 μ m.

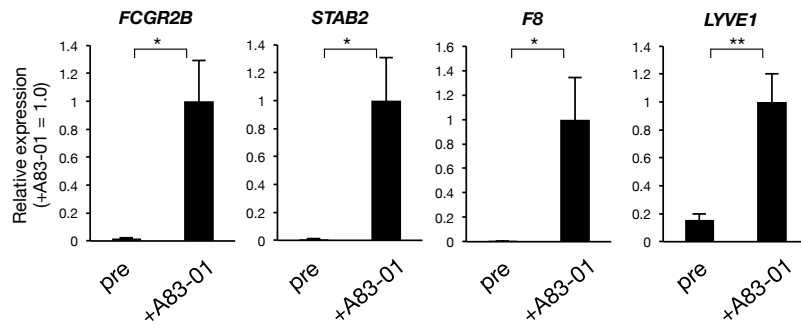


Figure 15. The effect of A83-01 treatment on LSEC maturation

Expression levels of mature LSEC specific markers in FLK1⁺CD31⁺CD34⁺ LSEC progenitors after A83-01 treatment (+A83-01). FLK1⁺CD31⁺CD34⁺ LSEC progenitors before A83-01 treatment were used as a control (pre). The results are shown as the mean \pm SEM of 9 independent experiments (each experiment contains 2 technical replicates).

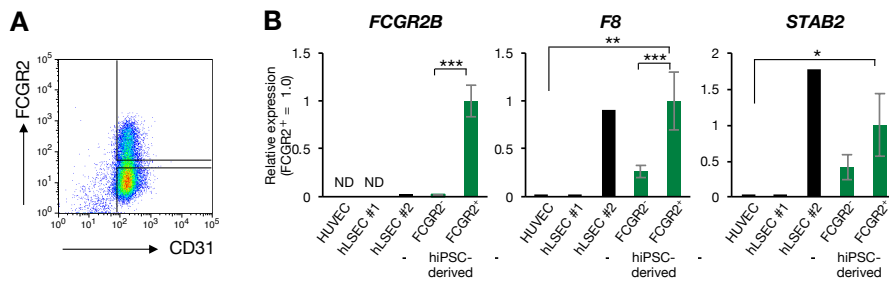


Figure 16. Expression of mature LSEC specific markers in hiPSC-derived LSECs

(A) FCM analysis of CD31 and FCGR2 in hiPSC-derived LSECs.

(B) Expression levels of the mature LSEC-specific marker genes (*FCGR2B*, *STAB2*, and *F8*) in HUVECs (n = 3), primary human LSECs (2 different lots, n = 1, 1), hiPSC-derived CD31⁺FCGR2⁻ cells (FCGR2⁻, n = 10), and CD31⁺FCGR2⁺ mature LSECs (FCGR2⁺, n = 10). The results shown are mean ± SEM of independent experiments (each experiment contains 2 technical replicates). *p < 0.05, **p < 0.01, ***p < 0.001. ND, not detected.

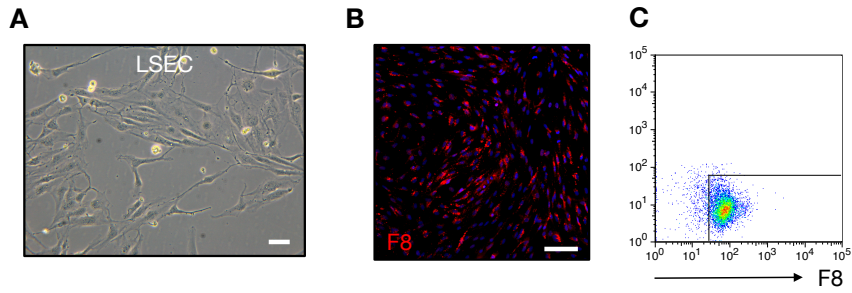


Figure 17. Characteristics of hiPSC-derived mature LSECs

(A) Phase-contrast image of CD31⁺FCGR2⁺ mature LSECs. Scale bar, 100 μ m.

(B) Immunofluorescence staining for F8 (red) in mature LSECs. Nuclei were counterstained with Hoechst 33342 (blue). Scale bar, 100 μ m.

(C) FCM analysis of Factor VIII (F8) in hiPSC-derived C CD31⁺FCGR2⁺ LSECs. Positive gates are defined by the isotype control.

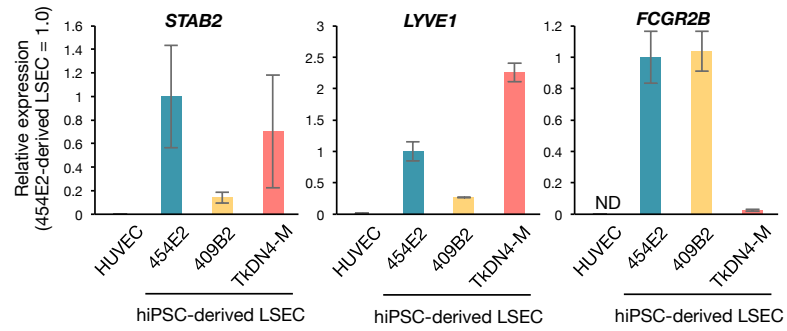


Figure 18. Characteristics of mature LSECs derived from multiple iPSC cell lines

Expression levels of LSEC marker genes in 454E2, 409B2, and TkDN4-M iPSC-derived LSECs. (n = 10, 3, 3). HUVECs were used as a control (n = 3). The results shown are mean \pm SEM of independent experiments (each experiment contains 2 technical replicates). ND: not detected.

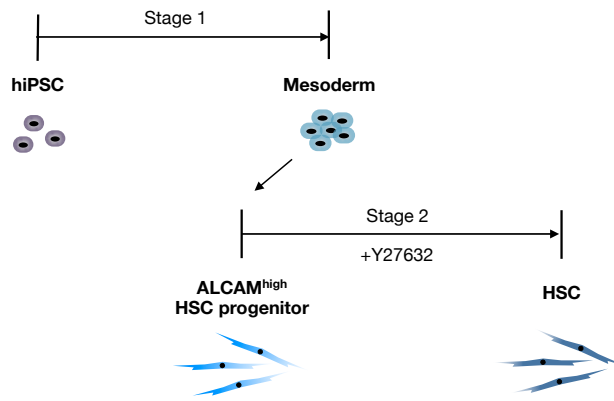


Figure 19. HSC differentiation from hiPSCs

Schematic representation of HSC differentiation from hiPSCs.

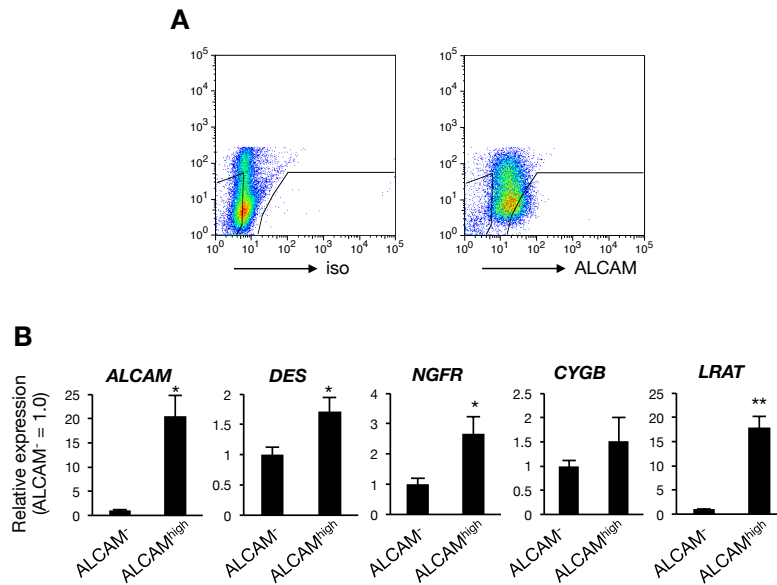


Figure 20. Isolation of hiPSC-derived HSC progenitors

(A) FCM analysis of ALCAM in hiPSC-derived mesodermal cells. The positive gate was defined by the isotype control.

(B) Expression levels of HSC markers in hiPSC-derived ALCAM^{high} HSC progenitors (ALCAM^{high}) compared with ALCAM⁻ cells (ALCAM⁻). The results are shown as the mean \pm SEM of 4 independent experiments (each experiment contains 2 technical replicates). * $p < 0.05$, ** $p < 0.01$.

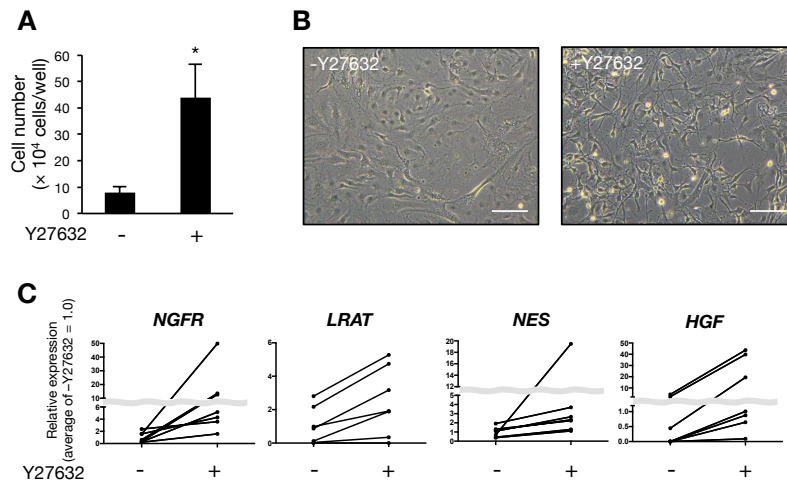


Figure 21. The effect of Y27632 treatment on HSC differentiation

(A) Growth of ALCAM^{high} HSC progenitors in culture with or without Y27632 treatment for 5 days. The results are shown as the mean \pm SEM of 3 independent experiments. * $p < 0.05$.

(B) Phase-contrast image of hiPSC-derived HSCs with or without Y27632 treatment after 5 days of culture. Scale bars, 100 μ m.

(C) Expression levels of the mature HSC marker genes (*NGFR*, *LRAT*, *NES*, and *HGF*) in hiPSC-derived HSCs (iPS-HSC) with or without Y27632 treatment ($n = 7$). Gene expression was compared between paired samples. Each experiment contains 2 technical replicates.

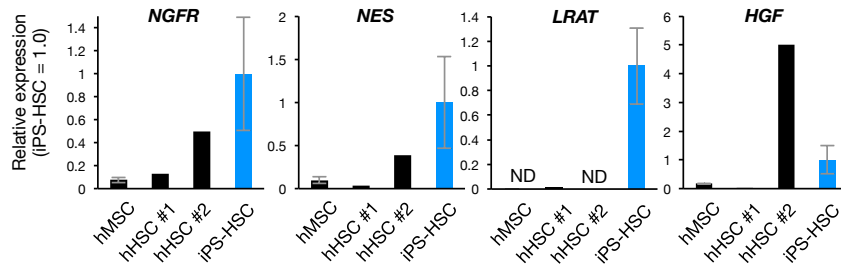


Figure 22. Expression of mature HSC specific markers in hiPSC-derived HSCs

Expression levels of the mature HSC marker genes (*NGFR*, *LRAT*, *NES*, and *HGF*) in hiPSC-derived HSCs (iPS-HSC) with Y27632 treatment (n = 7). Human MSCs (hMSC, n = 3) and primary human HSCs (2 different lots, n = 1, 1) were used as a control. The results shown are mean ± SEM of independent experiments (each experiment contains 2 technical replicates). ND: not detected.

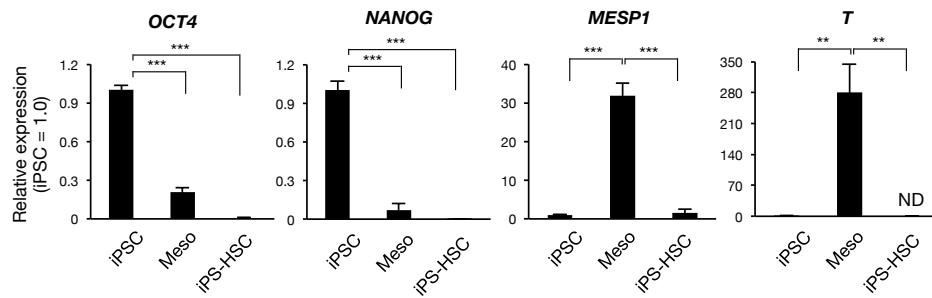


Figure 23. Gene expression of stage specific markers during HSC differentiation

Expression levels of pluripotent marker gene and mesodermal marker gene in hiPSCs (iPSC), hiPSC-derived mesodermal cells (Meso), hiPSC-derived HSCs (iPS-HSC). The results are shown as the mean \pm SEM of independent experiments (each experiment contains 2 technical replicates). n = 3, 5, 4 in each group. **p < 0.01, ***p < 0.001.

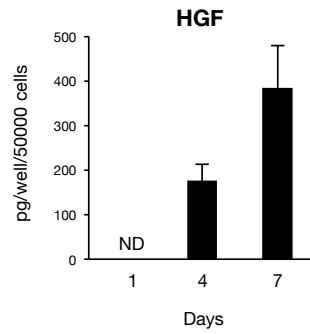


Figure 24. Characteristics of hiPSC-derived mature HSCs

Secretion levels of HGF during 1 day, 3 days, or 7 days in hiPSC-derived HSCs. The results are shown as the mean \pm SEM of 3 independent experiments. ND: not detected.

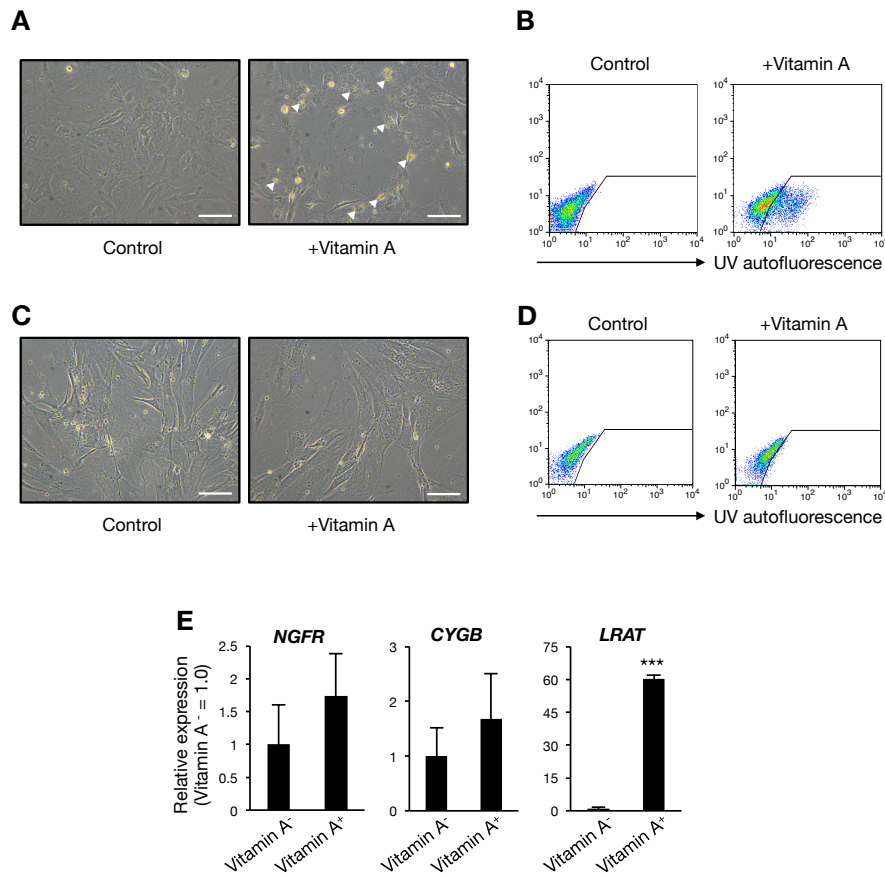


Figure 25. Vitamin A storage activity in hiPSC-derived HSCs

(A) Phase-contrast image of hiPSC-derived HSCs incubated with retinol (vitamin A). Arrowheads indicate droplets of vitamin A. Scale bars, 100 μ m.

(B) FCM analysis autofluorescence of intracellular vitamin A droplets in hiPSC-derived HSCs.

(C) Phase contrast image of human MSCs incubated with retinol (Vitamin A). Scale bars, 100 μ m.

(D) FCM analysis was performed in human MSCs against autofluorescence of intracellular Vitamin A droplets.

(E) Expression levels of the mature HSC marker genes in Vitamin A-stored hiPSC-derived HSCs (Vitamin A⁺). Vitamin A⁻ cells are used as control. The results are shown as the mean \pm SEM of 3 independent experiments (each experiment contains 2 technical replicates). *** $p < 0.001$.

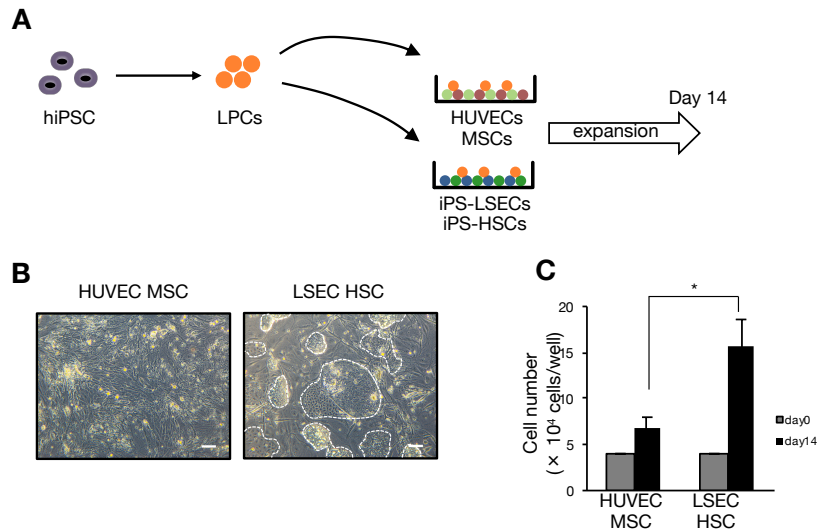


Figure 26. Co-culture of hiPSC-derived LPCs and NPCs

(A) Schematic representation of a co-culture system of hiPSC-derived liver cells.

(B) Phase-contrast image of hiPSC-derived CPM⁺ LPCs on HUVEC/MSC feeder cells (left) or hiPSC-derived NPC feeder cells (right) at day 14. White dashed lines outline colonies of CPM⁺ hepatoblasts. Scale bars, 100 μ m.

(C) Growth of CPM⁺ LPCs in culture for 14 days. The number of feeder cells was subtracted from total cell number in each well. The results are shown as the mean \pm SEM of 3 independent experiments. *p < 0.05.

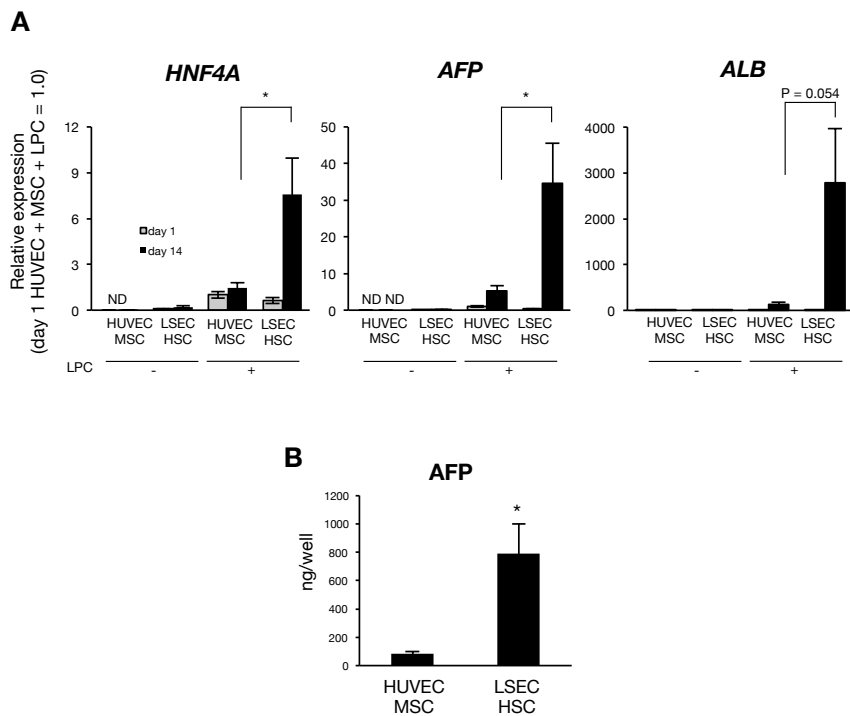


Figure 27. Characteristics of hiPSC-derived LPCs cultured on hiPSC-derived NPC feeder cells

(A) Expression levels of the LPC marker genes at day 1 and day 14 in CPM⁺ LPCs cultured on HUVEC/MSC feeder cells or hiPSC-derived NPC feeder cells (LSEC/HSC). The results are shown as the mean \pm SEM of 9 independent experiments (each experiment contains 2 technical replicates). * $p < 0.05$. ND: not detected.

(B) Secretion of AFP in hiPSC-derived LPCs on HUVEC/MSC feeder cells or hiPSC-derived NPC feeder cells (LSEC/HSC). The results are shown as the mean \pm SEM of 8 independent experiments. * $p < 0.05$.

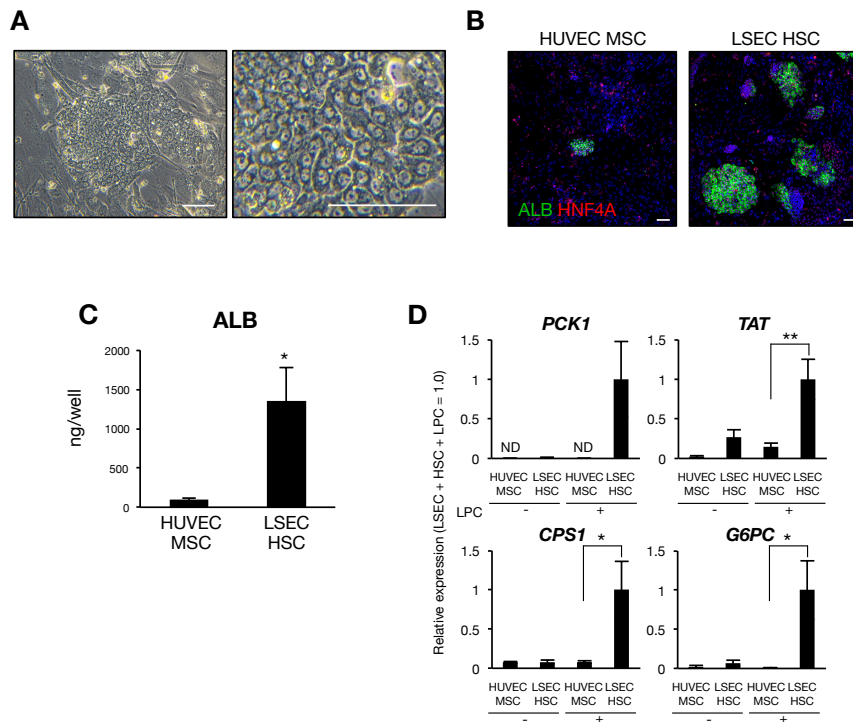


Figure 28. Characteristics of hiPSC-derived hepatocyte cultured on hiPSC-derived NPCs

(A) Phase-contrast image of hiPSC-derived hepatocytes on hiPSC-derived NPC feeder cells after induction of hepatic maturation. Scale bars, 100 μ m.

(B) Immunofluorescence staining for ALB (green) and HNF4A (red) in hiPSC-derived hepatocytes on HUVEC/MSC feeder cells or hiPSC-derived NPC feeder cells after induction of hepatic maturation. Nuclei were counterstained with Hoechst 33342 (blue). Scale bars, 100 μ m.

(C) Secretion of ALB in hiPSC-derived hepatocytes on HUVEC/MSC feeder cells or hiPSC-derived NPC feeder cells. The results are shown as the mean \pm SEM of 7 independent experiments. * $p < 0.05$.

(D) Expression levels of the metabolic enzyme genes after OSM stimulation in hiPSC-derived hepatocyte cultured on HUVEC/MSC feeder cells or hiPSC-derived NPC feeder cells (LSEC/HSC). The results are shown as the mean \pm SEM of 10 independent experiments (each experiment contains 2 technical replicates). * $p < 0.05$, ** $p < 0.01$.

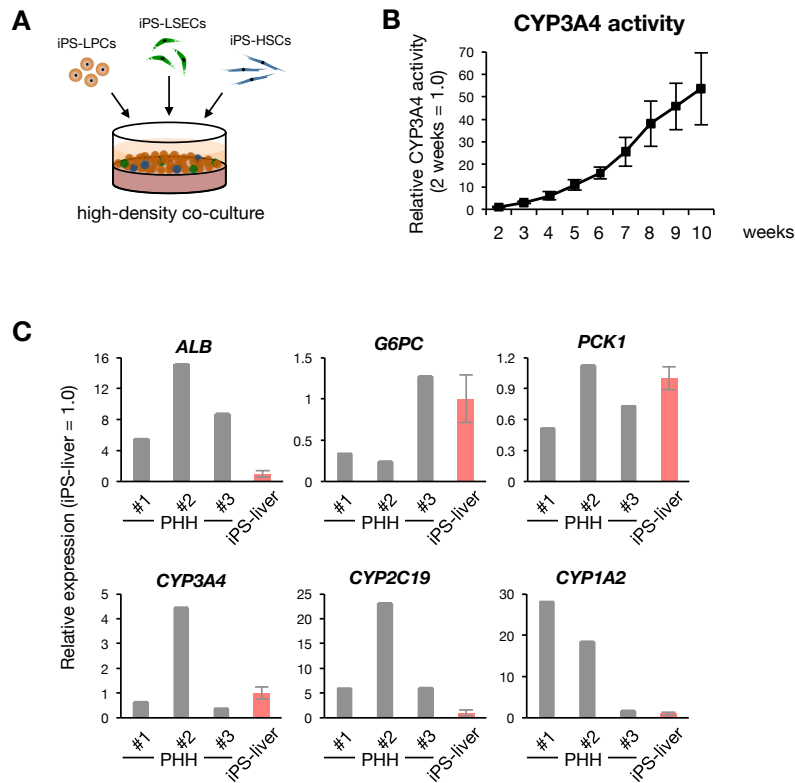


Figure 29. High-density co-culture system of hiPSC-derived liver cells

(A) Schematic representation of a high-density co-culture system of hiPSC-derived liver cells.

(B) Relative Cytochrome P450 3A4 (CYP3A4) activity in iPSC-derived liver cells. The results are shown as the mean \pm SEM of 3 independent experiments. The measurements were performed every week.

(C) Expression levels of mature hepatocyte marker genes after induction of terminal hepatic differentiation in hiPSC-derived liver cells (iPS-liver) (n = 3). Human primary cultured hepatocytes were used as control (PHH, 3 different donors). The results are shown as the mean \pm SEM (each experiment contains 2 technical replicates).

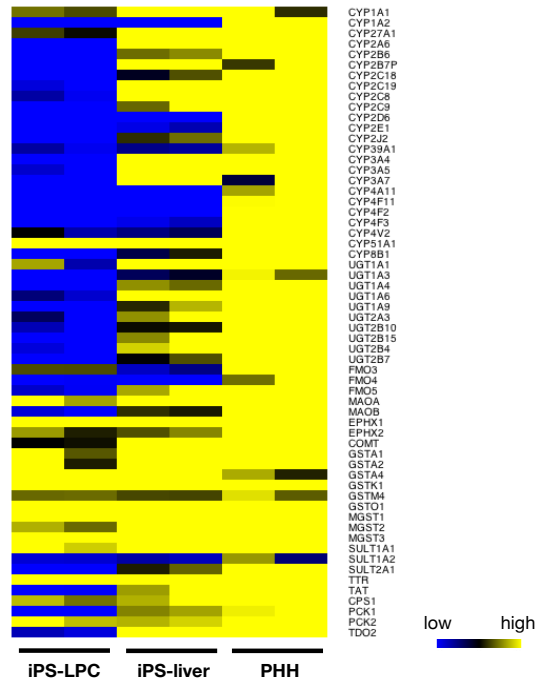


Figure 30. Comprehensive gene expression analysis of the hiPSC-derived liver model

Comparison of gene expression levels of hepatic metabolic enzyme genes in hiPSC-derived LPCs (iPS-LPC), hiPSC-derived liver model (iPS-liver), and primary human hepatocytes (PHH) by RNA-seq. Results of RNA-seq are depicted by color (n = 2, 2, 2).

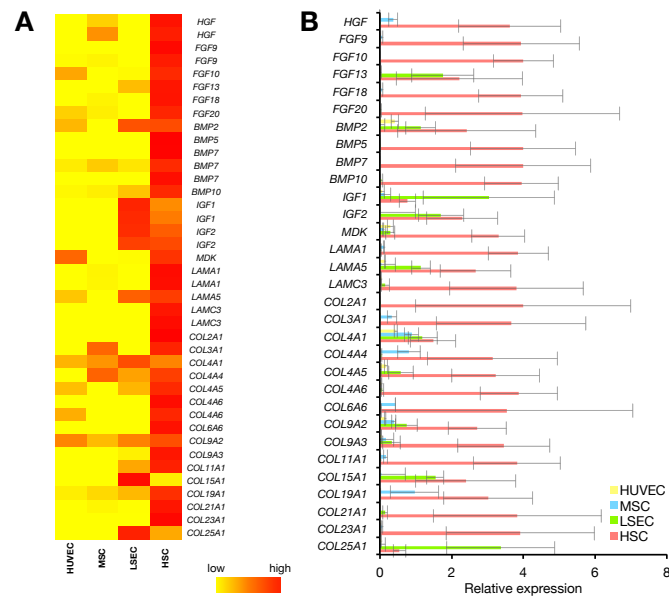


Figure 31. Gene expression levels of hepatic mitogens and extra cellular matrix in hiPSC-derived NPCs

(A) Comparison of gene expression levels of hepatic mitogens and extra cellular matrix related to liver development in HUVECs, MSCs, hiPSC-derived LSECs, and hiPSC-derived HSCs by microarray analysis. Results are depicted by color (n = 1).

(B) Comparison of gene expression levels of hepatic mitogens and extra cellular matrix related to liver development in HUVECs, MSCs, hiPSC-derived LSECs, and hiPSC-derived HSCs by qRT-PCR analysis. Results are shown as the mean \pm SEM of independent experiments (each experiment contains 2 technical replicates) (right). n = 3, 3, 3, 4 in each group.

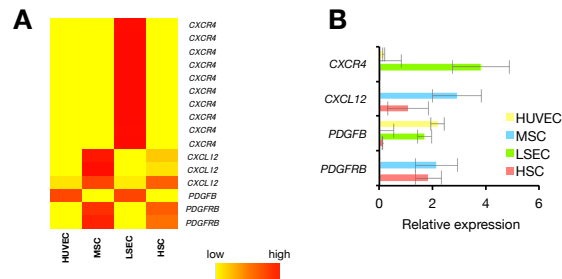


Figure 32. Gene expression levels related to vasculogenesis in hiPSC-derived NPCs

(A) Comparison of gene expression levels related to vasculogenesis in HUVECs, MSCs, hiPSC-derived LSECs, and hiPSC-derived HSCs by microarray analysis. Results of expression levels are depicted by color (n = 1).

(B) Comparison of gene expression levels related to vasculogenesis in HUVECs, MSCs, hiPSC-derived LSECs, and hiPSC-derived HSCs by qRT-PCR analysis. Results are shown as the mean \pm SEM of independent experiments (each experiment contains 2 technical replicates). n = 3, 3, 3, 4 in each group.

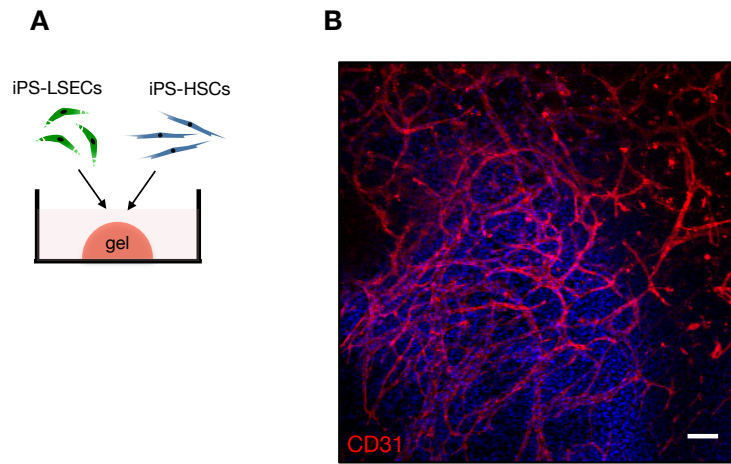


Figure 33. Three-dimensional co-culture system of hiPSC-derived LSECs and HSCs

(A) Schematic representation of a co-culture system of hiPSC-derived LSECs and HSCs.

(B) Immunofluorescence analysis for CD31 (red) in hiPSC-derived mature LSECs after induction of vasculogenesis with iPSC-derived HSCs. Nuclei were counterstained with Hoechst 33342 (blue). Scale bars, 100 μm .

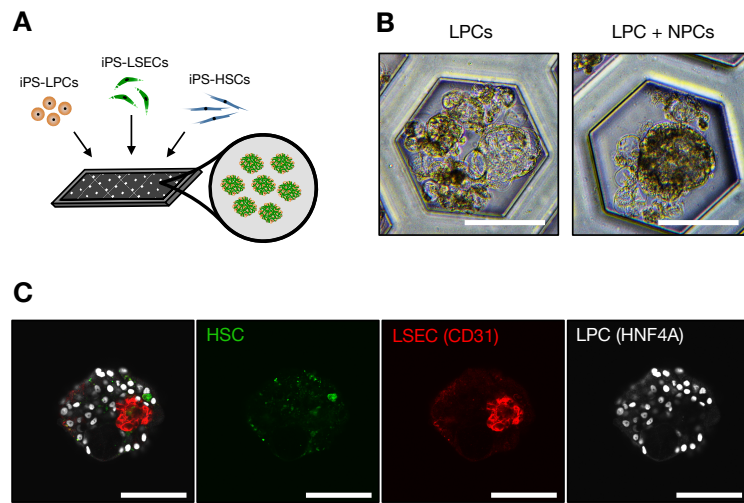


Figure 34. Three-dimensional co-culture system of hiPSC-derived LPCs and NPCs

(A) Schematic representation of a three-dimensional co-culture system of hiPSC-derived LPCs and NPCs.

(B) Phase-contrast image of hiPSC-derived LPCs without co-culture or with co-culture of NPCs in three-dimensional culture system. Scale bars, 100 μm .

(C) Immunofluorescence analysis for CD31 (red) and HNF4A (gray) in hiPSC-derived liver spheroids. HSCs are labeled with PKH linker kit (green). Nuclei were counterstained with Hoechst 33342 (blue). Scale bars, 100 μm .

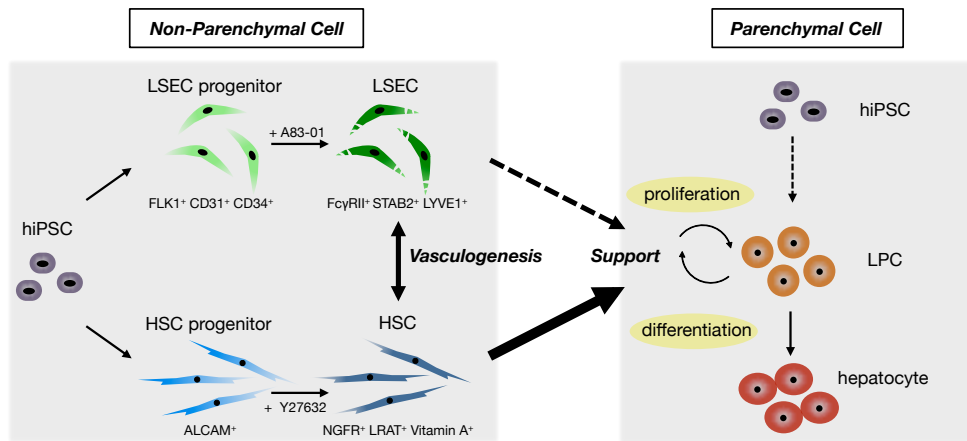


Figure 35. Conclusion of this study

Culture systems to generate LSECs and HSCs from human iPS cells. hiPSC-derived NPCs supported the proliferation and differentiation of hiPSC-derived LPCs. The co-culture system will be useful for disease models, drug screening and cell therapy.

Acknowledgments

I would like to thank my supervisor, Professor Atsushi Miyajima, Assistant Professor Taketomo Kido, and Professor Tatsuo Michiue for the thoughtful mentoring. I also would like to thank Naoko Miyata and Chizuko Koga for cell sorting, Noriko Imaizumi for mouse husbandry, Yoshiko Kamiya for technical assistance with experiments, and the member of the Miyajima lab for helpful discussion and advise. This study was supported by Japanese Society for the Promotion of Science (JSPS), Japan Agency for Medical Research and Development, and Graduate Program for Leaders in Life Innovation (GPLLI).